REGULAR PAPER

A dimensionality reduction approach in helicopter level flight performance testing

I. Arush[1] , M.D. Pavel[2] and M. Mulder[2]

[1]National Test Pilot School, Mojave, CA, 93502, USA and [2]Faculty of Aerospace Engineering, Delft University of Technology, Delft, The Netherlands
Corresponding author: I. Arush; Email: iarush@ntps.edu

Abstract

Evaluation of the power required in level flight is essential to any new or modified helicopter performance flight-testing effort. The conventional flight-test method is based on an overly simplification of the induced and profile power components required for a helicopter in level flight. This simplistic approach incorporates several drawbacks that not only make execution of flight sorties inefficient and time consuming, but also compromise the level of accuracy achieved. This paper proposes an alternative flight-test method for evaluating the level-flight performance of a conventional helicopter while addressing and rectifying all identified deficiencies of the conventional method. The proposed method, referred to as the corrected-variables screening using dimensionality reduction (CVSDR), uses an original list of 36 corrected variables derived from basic dimensional analysis principles. This list of 36 corrected variables is reduced using tools of dimensionality reduction to keep only the most effective level-flight predictors. The CVSDR method is demonstrated and tested in this paper using flight-test data from a MBB BO-105 helicopter. It is shown that the CVSDR method predicts the power required for level flight about 21% more accurately than the conventional method while reducing the required flight time by an estimate of at least 60%. Unlike the conventional method, the CVSDR is not bounded by the high-speed approximation associated with the induced power estimation, therefore it is also relevant to the low airspeed regime. This low-airspeed relevancy allows the CVSDR method to bridge between the level-flight regime and the hover. Although demonstrated in this paper for a specific type of helicopter, the CVSDR method is applicable for level-flight performance flight testing of any type of conventional helicopter.

Nomenclature

A_d	Main-rotor disk area
b	Main-rotor number of blades
$\bar{c}$	Averaged chord length (main-rotor blades)
C_{d_0}	Zero-lift drag coefficient (main rotor blades)
$C_P = \frac{P}{\rho_a A_d (\omega R)^3}$	Coefficient of power (non-dimensional)
$C_W = \frac{W}{\rho_a A_d (\omega R)^2}$	Coefficient of weight (non-dimensional)
$\vec{E}_r \big|_i$	Prediction error vector; difference between model (i) to actual measured power
$\overline{E}_{R(j)}$	Mean of absolute power prediction errors for sortie (j)
f_e	Fuselage equivalent flat-plate area for drag
P	Total power required for level flight
P_a	Ambient air static pressure
P_o	Standard sea-level air pressure (14.7psi)
$r_{x,y}$	Linear correlation coefficient between two variables x, y
R	Main-rotor radius

R_{air}	Specific gas constant for air
S_{x_i}	Standard deviation in sampled variable X_i
t_i	Test statistics of model (i) prediction errors
T_a	Ambient air static temperature
T_o	Standard sea-level static air temperature (288.15K)
V_T	True airspeed
W	Helicopter gross weight
X_{cg}	Helicopter longitudinal centre of gravity location
$\{\gamma_i\}$	Generic multivariable polynomial coefficients
$\delta = P_a/P_0$	Static pressure ratio (non-dimensional)
$\theta = T_a/T_0$	Static temperature ratio (non-dimensional)
$\mu \equiv \dfrac{V_T}{\Omega R}$	Advance ratio (non-dimensional)
ρ_a	Ambient air static density
ρ_o	Standard sea-level static air density (1.225kg/m³)
$\sigma = \rho_a/\rho_0$	Static density ratio (non-dimensional)
$\sigma_{i(i=1,2,...,r)}$	Singular values of a generic matrix of rank 'r'
$\sigma_R = \dfrac{b\bar{c}}{\pi R}$	Main-rotor solidity ratio (non-dimensional)
ψ_i	Generic non-dimensional (ND) variable
ψ_i^*	Generic corrected variable (ND for a specific helicopter type)
Ω, ω	Main-rotor angular speed

1.0 Introduction

The helicopter spends most of its flying time in the level flight regime. The relative time while cruising varies based upon the type and the specific mission the helicopter was designed for. Porterfield and Alexander [1] analysed data from various types of helicopters and proclaimed that on average the helicopter spends 71% of its flight time in level flight. The FAA [2] provides different estimates for two exemplary turbine helicopters. The first example is a utility-business-type helicopter that is estimated to spend 61% of its flight time while cruising, and the second example presented is for a transport helicopter which is estimated to spend 73% of its flight time in level flight. Regardless of where this value for relative time spent in level flight truly resides, the helicopter spends most of its flight time while cruising.

The helicopter performance flight test team may be tasked to execute a level flight performance test campaign for various reasons; it might be for a limited-scope validation of existing performance charts for certification purposes; or it might be for the task of updating performance charts due to external configuration modification; or it even be required for a full-scope level flight performance campaign, for which a complete set of charts and/or tables is required to specify the level flight performance of a brand new helicopter type. Whatever the reason is, the performance flight test team has a need for an efficient and accurate method to evaluate the helicopter performance in level flight.

The conventional flight-test method for helicopter level flight performance is based on a simplification of the equation for the power required to sustain a helicopter in level flight. This method is thoroughly discussed in the literature [3–7] and is demonstrated in numerous flight test reports [8–10]. This method is further explained and demonstrated in Section 2 of the paper using flight-test data of a MBB BO-105 helicopter. Although widely used, common practice shows that this flight-testing method is inefficient, time consuming and includes few drawbacks that seriously compromise the accuracy of the empirical power model it yields. The following is a list of the main disadvantages of the conventional flight-testing method, a list thoroughly discussed in the next sections.

First, the conventional method reduces a multi-dimensional physical problem into a three non-dimensional variable one. The three non-dimensional variables are the coefficient of power, *Cp*, the

advance ratio, μ and the coefficient of weight, Cw. The conventional method provides no comprehensive tools for addressing the effect of rotor blades compressibility on the power required for level flight. Boirun [11] addresses the compressibility effect in his work but his approach does not determine a decisive *unified* empirical model to include compressibility effects. Instead, various curves for different values of main-rotor tip Mach numbers are presented in the format of a carpet plot. Obtaining an accurate and unified empirical model to predict the level flight performance is highly desirable since it can also be easily used and implemented for real-time applications.

Second, the current method requires executions of various airspeed runs at constant coefficients of weight (Cw). This requirement makes the method inefficient, cumbersome and time consuming. Moreover, the resulting empirical model is prone to elevated levels of inaccuracy since it is merely a set of single power curves for constant Cw, rather than a unified empirical model, which accounts for the entire range of coefficients of weight.

Third, the conventional method takes the high-speed approximation for which the induced velocity of the air through the main-rotor disk is assumed negligible compared to the airspeed the helicopter flies at. By adopting this approximation, the conventional method becomes irrelevant for the low airspeed regime.

Fourth, the current method has no analytical means to account for the helicopter centre of gravity location although numerous flight-test campaigns show substantial dependency between the helicopter longitudinal centre of gravity and the power required for level flight. For example, Buckanin et al. [9] present an increase of about 10 square-feet in the equivalent flat-plate drag area of a Blackhawk helicopter resulting from a 15 inches forward migration of the centre of gravity in level flight.

Finally, the conventional method requires the flight test crew to precisely control the main rotor-speed. This requirement makes the current flight-test method unsuitable for helicopters for which their main-rotor speed control system cannot be easily overridden by the pilot.

Arush et al. [12–14] presented an alternative approach to helicopter performance flight testing, using multivariable polynomials as empirical models. This approach was proven more accurate (in excess of 300%) in the prediction of the available power of a helicopter under a wide range of atmospheric conditions, as compared to the conventional flight test method [12]. This multivariable approach was also used successfully in the prediction of the helicopter hover performance [13]. Taking this multivariable approach reduced the average prediction error by about 47% compared to the conventional flight test method for hover performance. The systematic procedure to screen between candidate multivariable predictors is discussed in Ref. [14]. The goal of the current paper is to implement this multivariable polynomial approach for the greater benefit of improving the level-flight test method. The proposed CVSDR method is aimed at addressing all identified drawbacks of the conventional method, specified as items (1) to (5) above, while providing an even more accurate prediction for power required in level flight. The CVSDR method is expanded to accommodate a more complicated helicopter performance problem than the hover performance [13]. Abstractly, the current paper can be regarded as a rigorous expansion of hover CVSDR method into a higher dimensional space of level-flight performance.

The paper is structured as follows: after the short introduction, the conventional flight-test method for level-flight performance is explained and demonstrated by using flight-test data from a MBB BO-105 helicopter. Flight-test data obtained from four distinct sorties totaling 44 data points are used to generate four empirical models. Each empirical model is then used to predict the power required for the other three sorties. This process is implemented for evaluating the level of accuracy one can expect by using the conventional flight-test method. Next, in Section 3, an alternative analysis to the CVSDR method is proposed. This method is demonstrated by using the same flight-test data used with the conventional method. In Section 4, the level of accuracy achieved using the proposed CVSDR method is analysed. This analysis includes all four sorties used with the conventional method and another sortie (number five) that was executed under arbitrary conditions for which the conventional method does not apply. Section 5 of this paper provides a comprehensive comparison between the conventional and the proposed CVSDR methods. Final conclusions and recommendations complete the paper.

2.0 The conventional flight-test method for level-flight performance

2.1 Introduction

The conventional flight-test method for determining level-flight performance of a helicopter is based on finding an empirical relationship between the coefficient of power (Cp) and the advance ratio of the helicopter (μ) for various discrete values of the coefficient of weight (Cw). This method is thoroughly discussed in the literature [3–7] and is derived from the fundamental equation to describe the components of power in level-flight (see Equation (1)). The power required for level flight is composed out of three main components: (1) the induced power required to overcome the induced drag of the main rotor blades; (2) the profile power required to compensate for the profile drag between the main and tail rotor blades and the air; and (3) the parasitic power required to overcome the drag between the fuselage of the helicopter and the air.

$$P = \underbrace{\frac{W^2}{2\rho_a A_d V_T}}_{induced} + \underbrace{\frac{1}{8} C_{d_0} \sigma_R \rho_a A_d (\Omega R)^3 \left(1 + k\mu^2\right)}_{profile} + \underbrace{\frac{1}{2} \rho_a f_e V_T^3}_{parasite} \therefore \mu \equiv \frac{V_T}{\Omega R}. \tag{1}$$

The induced power component in Equation (1) is assumed equal with the ideal power based on Glauert's high-speed approximation, which assumes the induced velocity through the main rotor is negligible compared to the airspeed the helicopter is flying at. This high-speed term is vaguely defined as it depends on the specific helicopter disk-loading, ambient atmospheric conditions, and the targeted error budget. For standard-day conditions and 2% estimation error, the high-speed approximation for a 3,000 pound Bell Jet-Ranger helicopter should be valid for airspeed above 33Kn. However, for a 42,000 pound Sikorsky CH-53D helicopter this approximation should be valid only for airspeeds of 61Kn and above. The significance of this high-speed approximation is that the current flight-test method is *irrelevant* to the low airspeed regime of the helicopter. Flight-test campaigns for level flight performance intentionally omit the low airspeed regime due to this reasoning and focus on the high-speed regime, which starts from a fairly vague airspeed value.

The profile power component in Equation (1) is merely an extension of the one estimated for the hover but with a correction term making it relevant for the level-flight regime. The coefficient (k) is multiplied by the advance ratio squared (μ^2) to represent the increase in profile power at level flight. The numerical values for this correction coefficient (k) were retrieved experimentally and vary between 4.65 (Refs. [3–6]) to 4.7 (Ref. [7]). The profile power component also assumes constant profile drag coefficient (Cd_0). This assumption breaks down in the presence of compressibility effects. References [15–17] provide various empirical models to represent the increase in the profile drag coefficient once the tip of the advancing blade reached the drag divergence Mach number. It is evident the current flight-test method, based on Equation (1), comprises considerable estimation inaccuracies for high altitude and low ambient temperatures, for which compressibility effects are more dominant.

Next, Equation (1) is normalised using $(\rho A_d (\Omega R)^3)$ to yield a non-dimensional equation (Equation (2)) which uses Cp, Cw and μ.

$$C_P = \frac{C_W^2}{2\mu} + \frac{1}{8} C_{d_0} \sigma_R \left(1 + k\mu^2\right) + \frac{1}{2} \frac{f_e}{A_d} \mu^3 \therefore C_P \equiv \frac{P}{\rho_a A_d (\Omega R)^3} \therefore C_W \equiv \frac{W}{\rho_a A_d (\Omega R)^2}. \tag{2}$$

The coefficient of power is now dependent on only two variables – the coefficient of weight and the advance-ratio. The conventional method seeks to simplify this non-dimensional relation even furthermore. This three-variable relation is reduced into sets of two-variable relations by presenting various coefficients of power to advance-ratio curves as measured at constant values of coefficient of weights. This requires the flight-test crew to execute speed runs while maintaining a constant coefficient of weight. Keeping a constant coefficient of weight during a speed run can be achieved in one of the following two ways:

(1) The foremost popular method is the constant weight over sigma, W/σ. In this method the flight-test crew maintains the coefficient of weight at a certain value by keeping a constant angular

speed of the rotor and maintaining the weight over relative density constant by adjusting the cruise altitude as the helicopter becomes lighter with the burn of fuel. This constant W/σ method is demonstrated mathematically as Equation (3).

$$C_W \equiv \frac{W}{\rho_a A_d (\Omega R)^2} = \frac{W}{\sigma \rho_o A_d (\Omega R)^2} = \underbrace{\frac{W}{\sigma} \cdot \frac{1}{\Omega^2}}_{held\ fixed} \cdot \frac{1}{\rho_o A_d R} \quad \therefore \sigma \equiv \frac{\rho_a}{\rho_o}. \tag{3}$$

The precise altitude change in between test points is calculated in real time by the test crew. This flight-test method is cumbersome in nature and makes the level flight performance data gathering inefficient and time consuming.

(2) The second approach of maintaining the coefficient of weight at a constant value as the helicopter burns fuel and becomes lighter is known as the constant weight of delta, W/δ method. This method is demonstrated mathematically as Equation (4).

$$C_W \equiv \frac{W}{\rho_a A_d (\Omega R)^2} = \frac{W}{\left(\frac{\delta p_o}{R_{air} T_a}\right) A_d (\Omega R)^2} = \underbrace{\frac{W}{\delta} \cdot \frac{T_a}{\Omega^2}}_{held\ fixed} \cdot \frac{R_{air}}{p_o A_d R^2} \quad \therefore \delta \equiv \frac{p_a}{p_o} \quad \therefore \rho = \frac{\delta p_o}{R_{air} T_a}. \tag{4}$$

Using the equation of state, the ambient air density can be related to the static temperature, pressure and the specific gas constant for air. By holding a constant ratio of weight over relative air pressure (δ) and a constant ratio of static ambient temperature (T_a) over the angular rotor-speed squared (Ω^2), the flight-test crew can ensure a constant coefficient of weight for those speed runs. Again, a cumbersome method that makes the level flight performance data gathering inefficient and time consuming.

The conventional flight test method for level flight performance typically includes the execution of five sorties, each conducted at a different constant coefficient of weight. The various coefficient of weights should cover the entire certified flight envelope of the helicopter. For each coefficient of weight the power required for level flight is measured at eight different airspeeds (as a minimum). This is defined as a speed run at constant coefficient of weight. Since all data points for a speed run share the same coefficient of weight and the gross weight of the helicopter reduces as fuel is burnt, the flight-test crew needs to adjust the altitude accordingly. The desired altitude for the subsequent data point (while at the same speed run) is calculated in real time by the flight-test crew, and it is common to encounter few iterations before the accurate altitude is reached. The extent of altitude climb between consecutive data points relates directly to the fuel consumption of the helicopter and the efficiency of the flight-test crew to stabilise the helicopter in the desired conditions. This altitude climb is typically between a few tens to a few hundred of feet. Once the new altitude is reached, the pilot needs to stabilise the helicopter at the new airspeed and to validate (or to readjust) the main-rotor angular speed remains constant. Note that the pilot is required to stay on-conditions for the entire duration necessary for the engine(s) to reach thermal equilibrium, followed by the data gathering period of time.

This procedure illustrates how cumbersome and time consuming the conventional flight-test method is. For small size and light helicopters, such as the BO-105, it takes about 5min to obtain one data point. One should appreciate that out of those 5min, only about two are essential for engine(s) thermal equilibrium attaining and data gathering. There is about 60% of time wasted due to the inefficiency of the conventional flight test technique. The requirement of **at least** 8 data points (different airspeeds) for each constant Cw and evaluating five different values of coefficient-of-weight translates into **at least** 3h and 20min of flight. This time duration should be regarded as an optimistic estimation based on small-sized helicopters. Executing level flight performance flight-test campaign on a large and heavy helicopter might even double this time duration. Proposing an alternative flight-test method that eliminates the requirement for flying at constant coefficient of weight has the potential for saving **at least** 2h of flight time for the same amount of required data points (60%).

Table 1. *Summary of flight-test conditions for sorties 1 through 4*

Sortie #	Gross weight* [Lbs.]	Average long. C.G. [In.]	Pressure altitude* [ft.]	Ambient air* temp. [°C]	Cw range* [$\times 10^{-3}$]	Average Cw [$\times 10^{-3}$]
1	4,890–5,012	123.8	4,000–4,670	12 to 14	5.78–5.80	5.79
2	4,760–4,865	123.9	5,040–5,400	12	5.77–5.83	5.80
3	4,270–4,380	123.5	7,770–8,520	9 to 10	5.78–5.80	5.79
4	3,890–3,960	124.4	11,210–11,820	0 to 2	5.78–5.80	5.79

* values represent the range of change during the sortie.
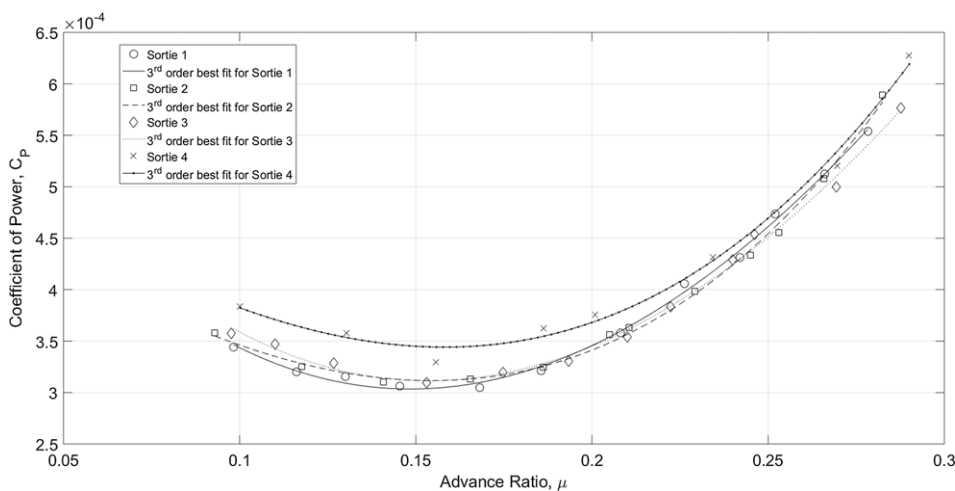
Figure 1. *Non-dimensional level flight performance of a MBB BO-105 helicopter (four distinct sorties).*

According to the current flight-test technique, as long as the helicopter flies straight and level at a constant Cw, its level flight performance can be uniquely represented by a single curve of Cp to μ. One should question how extensively can the single variables that constitute the coefficient of weight be varied, while keeping the coefficient of weight constant before an effect on the coefficient of power is noticeable. In other words, how realistic is the assumption on which the conventional level-flight test technique is built upon?

2.2 Example application

The conventional method is demonstrated within the context of deficiencies associated with the conventional method, using flight-test data obtained from a MBB BO-105 helicopter used for training at the National Test Pilot School (NTPS) in Mojave, CA. The power required to sustain level flight at various airspeeds was recorded during four distinct sorties. All four sorties, totaling 44 stabilised level flight points, were conducted at a targeted coefficient of weight (5.79×10^{-3}) with a tight tolerance between -0.3% to $+0.7\%$. The main rotor angular speed was kept constant at 100% (423 RPM) throughout the four sorties, as required by the conventional flight-test method. All physical values for gross-weights and atmospheric conditions are summarised in Table 1. Figure 1 presents all 44 data points of sorties 1 through 4 as matching pairs of Cp and μ accompanied with third-order polynomial best-fit curves.

The first concern to be discussed is the uniqueness of the Cp to μ curve for the four sorties executed. As previously noted, all four sorties were conducted at the same coefficient of weight and hence should all generate a unique Cp to μ curve. One can immediately doubt it just from observing Fig. 1. It seems quite evident that not all 44 flight-test data points belong to the same Cp to (μ) curve. As specified in Table 1 the Cw was held constant within a tight tolerance range of 1%. The expected variance in the

ΔCp due to the variance in Cw (ΔCw) can be estimated by a sensitivity analysis to Equation (2). This derivation is presented explicitly as Equation (5).

$$\Delta C_P = \frac{\partial C_P}{\partial C_W}(\Delta C_W) = \frac{\overline{C_W}}{\mu}(\Delta C_W) \therefore \overline{C_W} = 5.79 \times 10^{-3}. \tag{5}$$

From this analysis it is evident that the actual 1% variance in Cw should only be responsible for a ΔCp of 0.02%, under a high advance ratio of 0.3. For a low advance ratio of 0.1 the expected variance in Cp should reach up to only 0.06%. The actual variance in Cp during the four sorties reached 11% in low advance ratios of about 0.1, and 9% for high advance ratios of about 0.3. This variance in (Cp) cannot be entirely explained by the 1% variance in (Cw), therefore casting severe doubts on the soundness of this conventional flight-test method.

The level of accuracy achieved using the conventional flight-test method was assessed in two ways. The first and the foremost trivial assessment was to use each single sortie for the prediction of power required in each one of the other three sorties, then comparing the prediction to the actual power measured. This simplistic approach is addressed hereinafter as the ***single sortie approach***. The second approach for accuracy assessment was to base the power prediction of each sortie on a conglomerate of flight-test data from the other three sorties. This approach is referred-to hereinafter as the ***cluster of sorties approach***.

(1) ***The single-sortie approach:*** linear regressions were performed to retrieve four distinct third-order polynomials to describe the non-dimensional level-flight performance of the BO-105 helicopter for the particular tested coefficient of-weight (Equation (6)).

$$C_{P(j)} = a_3^j \mu^3 + a_2^j \mu^2 + a_1^j \mu + a_0^j \therefore j = 1, 2, 3, 4. \tag{6}$$

Each one of those four third-order polynomials ($C_{P(1)}$, $C_{P(2)}$, $C_{P(3)}$, *and* $C_{P(4)}$) was used to predict the power required for level flight under the conditions of the other three sorties. For example, the third-order polynomial based on Sortie 1 was used to predict power required for level flight under the conditions of sorties 2, 3 and 4. The third-order polynomial retrieved from Sortie 2 was used to estimate the power required for level flight under the conditions of sorties 1, 3 and 4 and so on. Power estimations were compared to the actual measured values and prediction errors for each data point were calculated as per Equation (7).

$$\vec{E}r_{(j)_i} = \left\{ C_{P(j)_i} - \left(a_3^j \mu_i^3 + a_2^j \mu_i^2 + a_1^j \mu_i + a_0^j \right) \right\} \rho_i A_d (\Omega_i R)^3 \therefore i = 1, 2, \ldots . \tag{7}$$

Figure 2 presents a summary of all prediction errors retrieved for all four sorties. These errors are presented in horse-power units and as a function of the corresponding μ. It is worth noting that positive prediction errors mean under estimation of the power required and a negative value represents an over estimation of power. From an operator standpoint, underestimation is the worst-case scenario since the helicopter demands for more power than predicted and planned for. This extra power needed might not be available from the engine(s), jeopardising a successful execution of the mission. On the other hand, overestimation of the power required can only contribute to inefficient planning and execution of the mission.

The prediction errors presented in Fig. 2 reveal a dissatisfying accuracy performance of the conventional method. For example, power prediction errors for Sortie 1 ranged between -20 hp (overestimate) to $+18$ hp (underestimate) using flight-test data from Sortie 2. Using flight-test data from Sortie 4 to predict power levels of Sortie 1 resulted in enormous overestimation errors that ranged between -50 and -2 hp. The means of the ***absolute*** prediction errors for each sortie were calculated as per Equation (8) and are presented in Fig. 3.
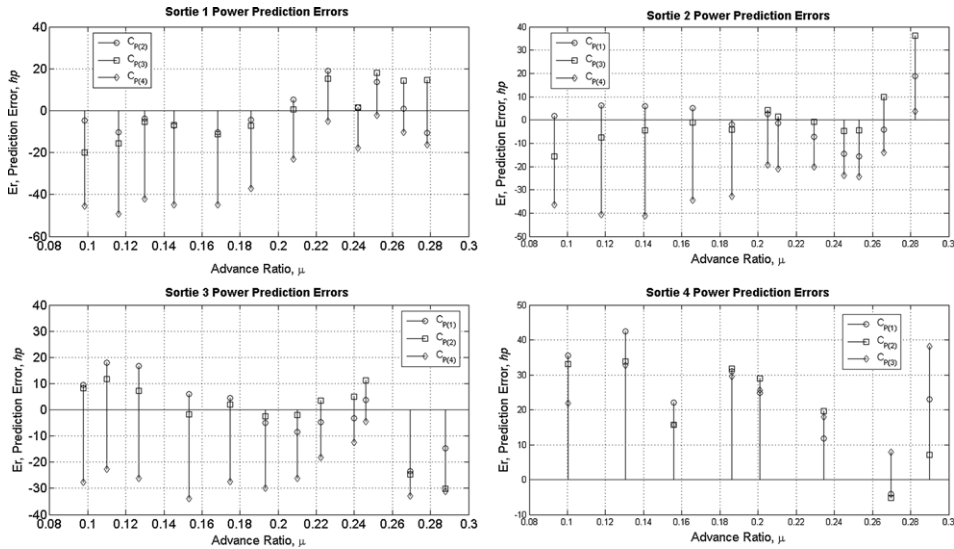
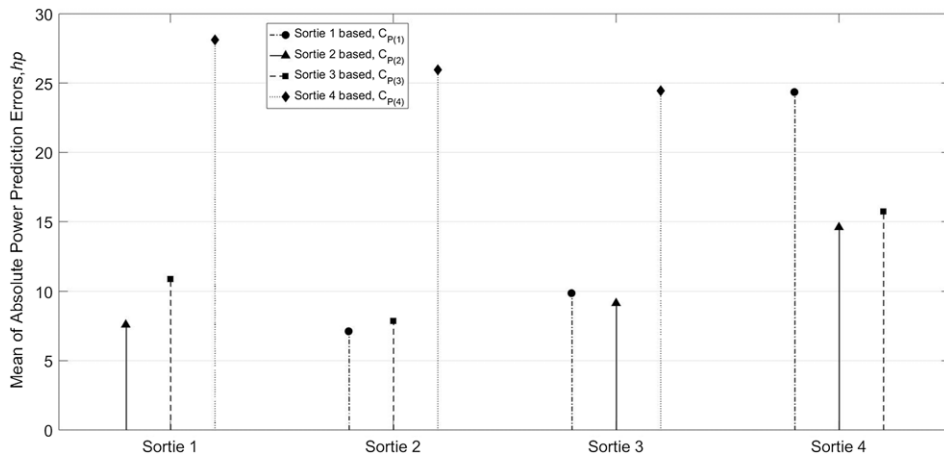**Figure 2.** *Power prediction errors for all four sorties (single-sortie approach).*

Figure 3. *Mean of absolute power prediction errors (single-sortie approach).*

$$\overline{E}_{R_{(j)}} = \frac{1}{n} \sum_{i=1}^{n} \left| E_{r(j)_i} \right| \qquad (8)$$

The **average** power prediction errors range from 7.2 to 28 hp and are considered by the authors unacceptable for the task of level flight power prediction. It is worth noting that for the specific type of helicopter tested, any power deviation above (or below) 4 hp from the expected value is clearly evident to the aircrew. The BO105 helicopter (like many other types of helicopters) is not equipped with an instrument that <u>explicitly</u> presents the engines output power in <u>hp units</u>; however, it is equipped with a torque-meter gauge (steam-gauge style), installed on the instrument panel, that indicates both engines output shaft torques. The smallest detectable resolution of this gauge translates into a 4 hp quantity.

One might debate whether these samples of prediction errors presented in Fig. 2 were drawn from a normally distributed population. For this, a quantile-quantile (QQ) plot is presented in Fig. 4. This plot compares the test data, the prediction errors samples in the case presented, to a theoretical sample
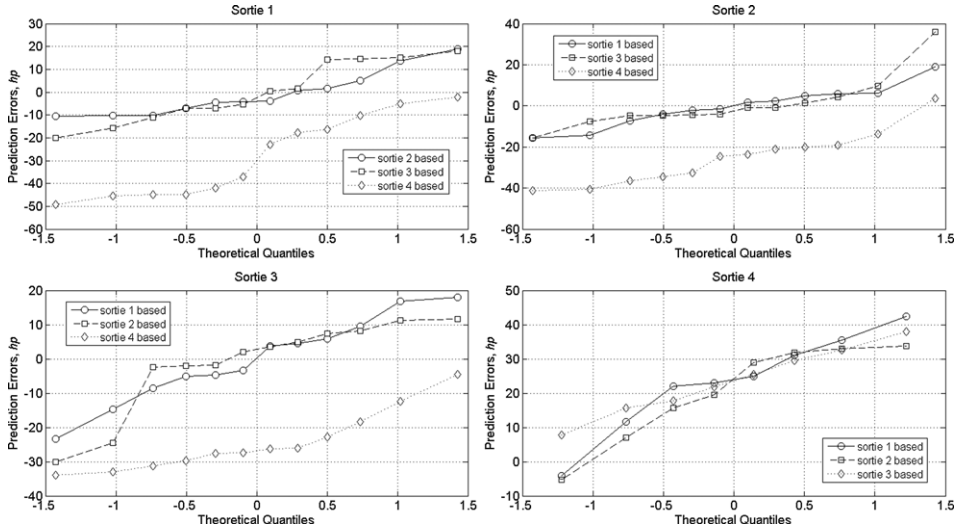
Figure 4. *Prediction errors quantiles to theoretical normal quantiles (QQ plot).*

drawn from a normally distributed population. A sample of data that comes from a normally distributed population would manifest itself as a straight line on the QQ plot. It is clear from Fig. 4 that all sampled prediction errors for sorties 1 through 4 do not come from a normally distributed population. Taking Sortie 1 as an example, the inflection of the curves might indicate that the largest (and smallest) estimate errors are not as extreme as would be expected in a normal distributed population. The QQ plots for Sortie 4 show a different behaviour than those of Sortie 1. The curves inflect in a way that might indicate heavier tails of the probability density function (PDF) as compared to a PDF of a normally distributed population. This means more extreme prediction errors are expected from both sides, underestimation and overestimation, compared to a normal distributed population.

The correlation between the power prediction level and the advance ratio was studied. For this, the correlation coefficient (r) between the prediction error and the advance ratio was calculated for each combination of sortie predicted and sortie used to base the empirical prediction model on. The correlation coefficient was calculated as per Equation (9), where (n) represents the number of data points (sample size) and (S) stands for the standard deviation of the sample.

$$r_{Er,\mu} = \frac{\frac{1}{n-1}\sum_{i=1}^{n}(Er \cdot \mu)_i - n \cdot \overline{Er} \cdot \overline{\mu}}{S_{Er}S_{\mu}}. \tag{9}$$

Figure 5 presents these correlation coefficients for all four Sorties. Sorties number 1, 2 and 3 had 12 data points and Sortie 4 had only 8. The sample size affects the correlation coefficient value to be considered significant. At the accustomed 95% confidence level and for a sample size of 12, a correlation coefficient of 0.58 (absolute value) and above indicates significant correlation between the two variables. For a smaller sample size of eight (Sortie 4), significant correlation between two variables (95% confidence level) is indicated by a correlation coefficient of 0.71 and above. Figure 5 clearly indicates a significant correlation between the power prediction errors and the advance ratio. The correlation value peaks when sorties 1 and 2 are used to predict the power levels of sorties 3 and 4 (and vice versa). The conclusion taken from this correlation analysis is there might be one (or few) latent dimensions, which is (are) missed by the conventional flight-test method. The empirical prediction models based on the conventional method fail to equally estimate power levels regardless of the advance ratio.
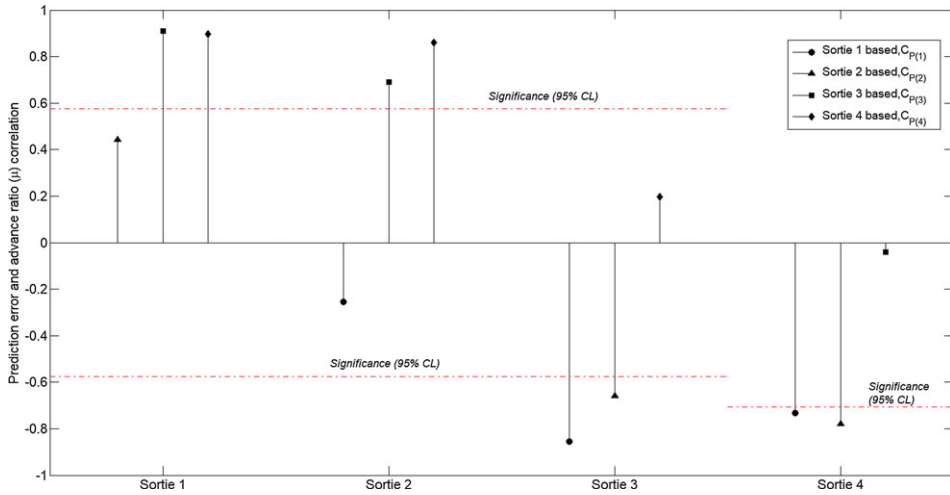
Figure 5. *Power prediction errors to advance ratio correlation (single-sortie approach).*
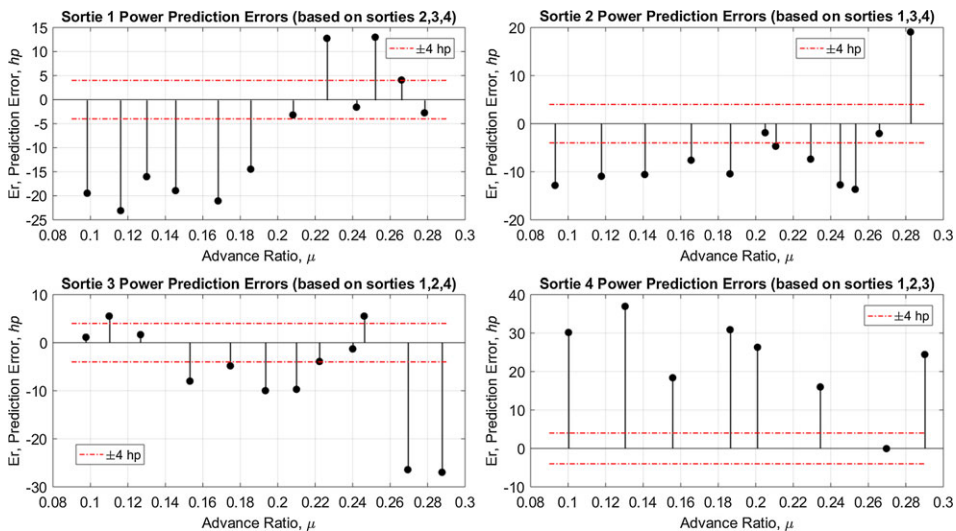

Figure 6. *Power prediction errors for all four sorties (cluster of sorties approach).*

(2) ***The cluster of sorties approach:*** similarly to the single-sortie approach, four linear regressions were performed to retrieve four distinct third-order polynomials to describe the non-dimensional level-flight performance of the BO-105 helicopter for the particular tested coefficient of weight (Equation (6)). The difference from the single-sortie approach is that data used for the regression was based on a conglomerate of three distinct sorties. Each one of these third-order polynomials was used to predict the power required for level flight under the conditions of the fourth sortie, the one not used for the linear regression. For example, data measured in sorties 1, 2 and 3 was used to regress a third-order polynomial, which was used to predict the power required of Sortie 4. Power estimation from each third-order polynomial were compared with the actual measured values and the estimation errors were calculated as per Equation (7). Figure 6 presents a summary of all prediction errors retrieved for all four sorties. The prediction errors are presented in horse-power units and as a function of the corresponding advance-ratio.
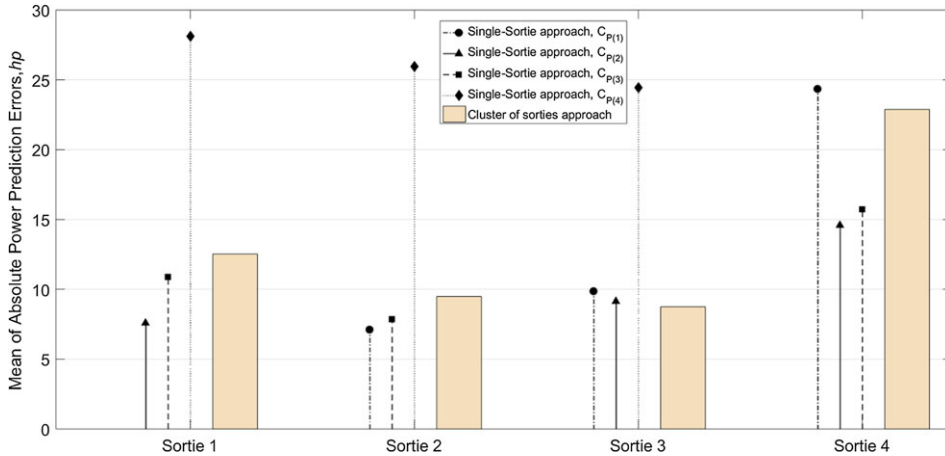
Figure 7. *Mean of absolute prediction errors – single-sortie and cluster of sorties comparison.*

Subscribing to the cluster of sorties approach slightly improves the prediction performance. The power prediction errors of Sortie 1 ranged from −23 hp (overestimate) to 13 hp (underestimate). Using flight test data measured in sorties 1, 3 and 4 to predict power levels of Sortie 2 yielded prediction errors between 14 and 19 hp. The power predictions errors for Sortie 3 ranged between −27 and 5.5 hp and power predictions for Sortie 4 were all underestimating the true measured power by up to 37 hp. The four means of the ***absolute*** prediction errors for each sortie were calculated as per Equation (8) and are presented in Fig. 7, alongside the absolute prediction errors yielded from the single-sortie approach (Fig. 3). The averaged absolute power prediction errors ranged between 8.8 and 22.9 hp (mean of 13.4 hp with a standard deviation of 6.5 hp).

One might ask how do those specific averaged prediction errors presented in Fig. 7 relate to the general case? The conventional approach in flight-testing for inferring from a particular test to the general case is based on hypothesis-testing. This approach, which follows from the central-limit theorem, is thoroughly discussed in the literature (Refs. [18, 19]). In a nutshell, a hypothesis is set (the null-hypothesis) and by using the test-statistics (Equation (10)) the validity of the null-hypothesis is assessed against the alternative hypothesis. For the specific case presented, the null-hypothesis assigned is that *on-average* the power required for level-flight as predicted by the conventional flight-test method (using the cluster-of-sorties approach) and the empirical model obtained (Equation (6)) does not differ from the true measured power by more than ±4 hp. This null hypothesis is tested against the alternative that *on-average* the power required for level-flight as estimated by the conventional method differ from the actual power by more than 4 hp (absolute value). The motivation for setting 4 hp as the threshold for the null-hypothesis is based on the reasoning that for the BO105 helicopter any power deviation above (or below) 4 hp is noticeable to the aircrew. As previously explained, the amount of power produced by the engines is (implicitly) presented to the aircrew by the engines torques meter gauge. The smallest detectable resolution of this gauge translates into a 4 hp quantity.

The relevant test statistic for this hypothesis testing is calculated per Equation (10). The symbol n represents the number of sorties and S stands for the standard deviation of the averaged power prediction errors which were calculated per Equation (8) and presented in Fig. 7.

$$t = \frac{\left|\bar{E}_r\right| - \eta_0}{S / \sqrt{n}} \therefore \eta_0 = 4 \, hp. \tag{10}$$

The calculated value for the test statistic was 2.89. Inferential statistical analysis shows the probability for making a Type-I error by rejecting the null hypothesis to be small (3%). This small probability for a Type-I error fall below the 5% significance level accustomed in helicopter performance flight testing.

The practicality of this test is that there is sufficient statistical evidence to reject the null hypothesis and to adopt the alternative hypothesis instead. There is practically no statistical evidence to support the null hypothesis assigned. Complementary statistical analysis shows that ***on-average*** and at the 95% confidence level, the level-flight power predictions based on the current method and Equation (6) deviate by ±5.8 hp from the actual measured power.

The poor power-prediction performance of the current flight-test method is to be expected. As discussed above, the current level-flight performance method assumes that for a constant coefficient of weight the coefficient of power is solely dependent on the advance ratio, regardless of any compressibility effects that might be present. Based on data and analysis presented above, this is clearly not a sound assumption to make. Another potential contributor to the unsatisfactory power prediction might be related to the change of the longitudinal centre of gravity. As mentioned in the introduction, a longitudinal migration in the centre of gravity should have an effect on the total drag area of the fuselage, hence affecting the power required for level flight.

The next section of the paper presents an alternative flight-test method for level-flight performance. This CVSDR method shows much improved prediction accuracy as compared to the current flight-test method. The CVSDR method also addresses all of the current method deficiencies as listed in the introduction section of the paper.

3.0 The corrected variables screening using dimensionality reduction method (CVSDR)

The CVSDR method aims to rectify all identified drawbacks of the existing method, while providing better prediction accuracy as compared to the conventional method. The CVSDR method is presented hereinafter in three phases. Employment of this method by flight testers will require recitation of only the last two phases since the first phase is generic to all conventional helicopters. Phase 1 deals with the generation of an original list of corrected variables for a multivariable analysis. In Phase 2 this list of corrected variables is refined based on concepts of dimensionality reduction. Phase 3 of the proposed method focuses on finding an empirical multivariable model using the bare-essential corrected variables (regressors) which were identified in Phase 2. This list of corrected variables serves as an orthogonal base for the specific helicopter level-flight performance. The complete CVSDR method is demonstrated using the same MBB BO-105 helicopter flight-test data, already presented in Section 2 of this paper. A practical and convenient summary of the method is presented in Section 3.4. This summary is intended to serve as a guide for the flight testers who wish to evaluate the power required for level flight of a conventional helicopter using the CVSDR method. This summary provides brief directions with regards to level-flight data base establishment and analysis.

3.1 Phase 1 – Generating an original list of corrected variables to represent the level-flight performance

The physical problem of the power required to sustain a helicopter in level-flight (out-of-ground effect) was reevaluated using tools of dimensional analysis (Refs. [20, 21]). The procedure starts by proposing variables that are expected to affect the power required in level flight. These are the ambient static pressure, P_a, the ambient static temperature, T_a, the helicopter gross weight, W, the true airspeed the helicopter flies at, V_T, the main-rotor disk area, A_d, the main rotor angular speed, ω and the longitudinal location of the centre of gravity, X_{cg}. The power required to hover, P, can be represented mathematically as Equations (11) and (12) in implicit form.

$$P = f(P_a, T_a, W, V_T, A_d, \omega, x_{cg}), \tag{11}$$

$$\hat{f}(P, P_a, T_a, W, V_T, A_d, \omega, x_{cg}) = 0. \tag{12}$$

The dimensions involved are presented in Table 2. *M* represents mass, *L* represents length and *T* represents time.

Table 2. *Summary of all variables and dimensions involved*

#	Physical variable	Notation	Dimension
1	Power required for level-flight	P	$[M][L]^2[T]^{-3}$
2	Ambient static pressure	P_a	$[M][L]^{-1}[T]^{-2}$
3	Ambient static temperature	T_a	$[L]^2[T]^{-2}$
4	Helicopter gross weight	W	$[M][L][T]^{-2}$
5	True airspeed	V_T	$[L][T]^{-1}$
6	Main-rotor disk area	A_d	$[L]^2$
7	Main-rotor angular speed	ω	$[T]^{-1}$
8	Longitudinal centre of gravity	X_{cg}	$[L]$

The physical problem of power required for level flight has eight variables involved with three dimensions (L, M, T). According to the Buckingham Pi-Theorem [20] the complexity of the problem can be reduced from eight dimensional variables to only five non-dimensional (ND) variables. Following the methodology presented by Buckingham [20] these five ND variables (denoted by ψ) are formed as products of the dimensional variables. Since there are eight dimensional variables to construct five ND variables, three dimensional variables were used as repeating variables in the ND products (ψ). There are 56 different options to choose three variables out of eight for the case where the order does not matter (combinations). That requires a fairly tedious task of screening among 56 different options in order to identify the best way of describing the non-dimensional level-flight performance. The following is a demonstration of only one combination out of the 56 options available. In this particular demonstration, the three repeating variables are the ambient static temperature (Ta), the helicopter gross weight (W) and the main rotor disk area (Ad). The five ND products (ψ) are defined in Equation (13). According to Buckingham [20], the repeating variables should be raised to some arbitrary powers, those are denoted as $a_1, b_1, c_1, \ldots, c_5$ in Equation (13). As demonstrated hereinafter, these arbitrary powers are identified as those numeric values that make the ψ products non-dimensional.

$$\begin{cases} \psi_i = (T_a)^{a_1}(W)^{b_1}(A_d)^{c_1}(P) \\ \psi_j = (T_a)^{a_2}(W)^{b_2}(A_d)^{c_2}(P_a) \\ \psi_k = (T_a)^{a_3}(W)^{b_3}(A_d)^{c_3}(\omega) \\ \psi_m = (T_a)^{a_4}(W)^{b_4}(A_d)^{c_4}(V_T) \\ \psi_n = (T_a)^{a_5}(W)^{b_5}(A_d)^{c_5}(x_{cg}) \end{cases} . \qquad (13)$$

Next, the procedure requires to replace each one of the dimensional variables with their corresponding dimensions and to enforce each one of the five ψ products to be non-dimensional. This process is demonstrated as per Equation (14). Each one of the ψ products yields three equations with three unknowns, which are the exponents. Solving for the exponents of ψ_i is demonstrated in Equation (15). The same process is then repeated for each one of the other ND variables, ψ_j, ψ_k, ψ_m and ψ_n.

$$\begin{cases} [\psi_i] = \left[\frac{L^2}{T^2}\right]^{a_1}\left[\frac{ML}{T^2}\right]^{b_1}[L^2]^{c_1}\left[\frac{ML^2}{T^3}\right] = M^{b_1+1}L^{2a_1+b_1+2c_1+2}\,T^{-2a_1-2b_1-3} \equiv M^0L^0T^0 \\[2mm] [\psi_j] = \left[\frac{L^2}{T^2}\right]^{a_2}\left[\frac{ML}{T^2}\right]^{b_2}[L^2]^{c_2}\left[\frac{M}{LT^2}\right] = M^{b_2+1}L^{2a_2+b_2+2c_2-1}\,T^{-2a_2-2b_2-2} \equiv M^0L^0T^0 \\[2mm] [\psi_k] = \left[\frac{L^2}{T^2}\right]^{a_3}\left[\frac{ML}{T^2}\right]^{b_3}[L^2]^{c_3}\left[\frac{1}{T}\right] = M^{b_3}L^{2a_3+b_3+2c_3}\,T^{-2a_3-2b_3-1} \equiv M^0L^0T^0 \\[2mm] [\psi_m] = \left[\frac{L^2}{T^2}\right]^{a_4}\left[\frac{ML}{T^2}\right]^{b_4}[L^2]^{c_4}\left[\frac{L}{T}\right] = M^{b_4}L^{2a_4+b_4+2c_4+1}\,T^{-2a_4-2b_4-1} \equiv M^0L^0T^0 \\[2mm] [\psi_n] = \left[\frac{L^2}{T^2}\right]^{a_5}\left[\frac{ML}{T^2}\right]^{b_5}[L^2]^{c_5}[L] = M^{b_5}L^{2a_5+b_5+2c_5+1}\,T^{-2a_5-2b_5} \equiv M^0L^0T^0 \end{cases}, \qquad (14)$$

$$\left.\begin{array}{l} [M]: b_1 + 1 = 0 \\ [L]: 2a_1 + b_1 + 2c_1 + 2 = 0 \\ [T]: -2a_1 - 2b_1 - 3 = 0 \end{array}\right\} \Rightarrow \begin{bmatrix} 0 & 1 & 0 \\ 2 & 1 & 2 \\ -2 & -2 & 0 \end{bmatrix} \begin{Bmatrix} a_1 \\ b_1 \\ c_1 \end{Bmatrix} = \begin{Bmatrix} -1 \\ -2 \\ 3 \end{Bmatrix} \Rightarrow \begin{Bmatrix} a_1 \\ b_1 \\ c_1 \end{Bmatrix} = \begin{Bmatrix} -1/2 \\ -1 \\ 0 \end{Bmatrix}. \tag{15}$$

Based on Equation (15) the first ND variable (ψ_i) can be written as Equation (16)

$$\psi_i = \frac{P}{W\sqrt{T_a}}. \tag{16}$$

This ND variable (Equation (16)) can be further simplified once the ambient static temperature is represented using its relative value (Equation (17)). This gives a simplified expression for ψ_i (Equation (18)) denoted as ψ_i^*. Since this term indeed carries dimensions and is not a pure ND, it is better defined as a corrected variable (CV).

$$P_a = P_0 \cdot \delta \therefore T_a = T_0 \cdot \theta, \tag{17}$$

$$\psi_i = \frac{P}{W\sqrt{T_a}} = \frac{P}{W\sqrt{T_0\theta}} = \frac{1}{\sqrt{T_0}} \cdot \frac{P}{W\sqrt{\theta}} = Const \cdot \frac{P}{W\sqrt{\theta}} \Rightarrow . \tag{18}$$

$$\psi_i^* = \frac{P}{W\sqrt{\theta}}$$

A similar analysis was conducted to reveal the other four ND variables (ψ_j, ψ_k, ψ_m and ψ_n). These ND variables were further simplified to represent non-dimensional variables of a particular helicopter, hence referred to as corrected-variables (CVs). The corresponding CVs are denoted with an asterisk and presented as Equation (19).

$$\psi_j^* = \frac{W}{\delta} \therefore \psi_k^* = \frac{\omega}{\sqrt{\theta}} \therefore \psi_m^* = \frac{V_T}{\sqrt{\theta}} \therefore \psi_n^* = \frac{X_{cg}}{R}. \tag{19}$$

The procedure demonstrated above was repeated for all other 55 possibilities of choosing three variables out of eight. From all 56 options evaluated, 20 did not yield a unique solution, and a few other returned repeating ND variables. Overall, the analysis yielded 36 distinct CVs that can be used for the helicopter level-flight performance. Table 3 summarises all 36 CVs in an array form to indicate which of the five dimensional variables (power, weight, true airspeed, main-rotor angular speed and\or longitudinal centre of gravity location) are used in the specific CV. This list of CVs is also presented graphically in Fig. 8, where one can clearly observe the number of dimensional variables involved in each CV. There are 6 CVs that are based on only one dimensional variable (1-D), 16 CVs that include two dimensional-variables (2-D), 13 CVs that employ three dimensional variables (3-D) and only 1 CV (ψ_{36}^*) which involves four dimensional variables (4-D).

3.2 Phase 2 – Screening for effective corrected-variables (CV) using dimensionality reduction

The second phase of the CVSDR method requires the evaluation of the list of 36 CVs (Table 3) and the determination of the most effective CVs in representing the level-flight performance of a specific helicopter. A power-based corrected variable needs to be expressed as a function of few other CVs. For this, the flight tester might be asking the following questions:

- How many CVs are required for a sufficient description of the level-flight performance?
- Which CVs should be used?

Table 3. *Corrected-variables (CVs) to represent the level-flight performance*

	Power based	M/R angular-speed based	Weight based	Airspeed based	C.G. based	Three-dimensional variables	Four-dimensional variables
Power based	$\psi_1^* = \dfrac{P}{\delta\sqrt{\theta}}$	$\psi_4^* = \dfrac{P}{\delta\omega}$	$\psi_5^* = \dfrac{P}{W\sqrt{\theta}}$	$\psi_{11}^* = \dfrac{P}{\delta V_T}$	$\psi_{22}^* = \dfrac{P}{X_{cg}^2\delta\sqrt{\theta^3}}$	$\psi_6^* = \dfrac{P}{\omega W}$	$\psi_{36}^* = \dfrac{P}{W\omega X_{cg}}$
		$\psi_7^* = \dfrac{P\omega^2}{\delta\sqrt{\theta^3}}$	$\psi_{12}^* = \dfrac{P}{W}$		$\psi_{23}^* = \dfrac{P}{X_{cg}^2\delta\sqrt{\theta}}$	$\psi_9^* = \dfrac{P\sqrt{\delta}}{\omega\sqrt{W^3}}$	
		$\psi_{20}^* = \dfrac{P}{\sqrt{\delta}\omega}$				$\psi_{25}^* = \dfrac{P}{WV_T}$	
		$\psi_{21}^* = \dfrac{P}{\omega^2\delta\sqrt{\theta^3}}$				$\psi_{26}^* = \dfrac{P\cdot\delta}{\omega\sqrt{W^3}}$	
		$\psi_{24}^* = \dfrac{1}{\theta}\sqrt[3]{\left(\dfrac{P\omega^2}{\delta}\right)^2}$				$\psi_{27}^* = \dfrac{V_T\sqrt{\delta}}{\omega\sqrt{W}}$	
M/R angular-speed based		$\psi_3^* = \dfrac{\omega}{\sqrt{\theta}}$	$\psi_8^* = \dfrac{W\omega^2}{\delta\theta}$	$\psi_{13}^* = \dfrac{V_T}{\omega}$	$\psi_{16}^* = \dfrac{X_{cg}}{\omega\sqrt{\theta}}$	$\psi_{28}^* = \dfrac{V_T\omega\sqrt{W}}{\sqrt{\delta}}$	
		$\psi_{14}^* = \omega^2\sqrt{\theta}$			$\psi_{17}^* = \dfrac{X_{cg}\omega}{\sqrt{\theta}}$	$\psi_{29}^* = \dfrac{P\omega}{\sqrt{\delta V_T^3}}$	

Table 3. *Continued*

	Power based	M/R angular-speed based	Weight based	Airspeed based	C.G. based	Three-dimensional variables	Four-dimensional variables
Weight based			$\psi_2^* = \dfrac{W}{\delta}$		$\psi_{18}^* = \dfrac{WX_{cg}^2}{\delta}$	$\psi_{30}^* = \dfrac{P\omega^2}{\delta V_T^3}$	
					$\psi_{19}^* = \dfrac{W}{\delta X_{cg}^2}$	$\psi_{31}^* = \dfrac{P}{\omega X_{cg}\theta}$	
Airspeed based				$\psi_{10}^* = \dfrac{V_T}{\sqrt{\theta}}$		$\psi_{32}^* = \dfrac{P}{\omega X_{cg}^3 \delta}$	
C.G. based					$\psi_{15}^* = \dfrac{X_{cg}}{R}$	$\psi_{33}^* = \dfrac{V_T}{\omega X_{cg}}$	
						$\psi_{34}^* = \dfrac{P}{V_T X_{cg}^2 \delta}$	
						$\psi_{35}^* = \dfrac{PV_T}{X_{cg}^2 \delta}$	

Figure 8. *Graphical presentation of all 36 CVs for the level-flight performance.*

These questions are addressed in this phase of the CVSDR method. The procedure of CVs selection, both the quantity and types of CVs, is based on principals of dimensionality reduction and the correlated mathematical procedure known as the singular value decomposition (SVD). This phase of the method is demonstrated using the same MBB BO-105 level-flight test data presented in Section 2 above.

The SVD theorem

The theory and mechanics of the SVD are thoroughly discussed in literature [22]. In a nutshell, this theorem states that any matrix from any size that holds real numbers as entries can be decomposed as a product of three unique and special matrices, as shown in Equation (20).

$$Z = U\Sigma V^T = \begin{bmatrix} u_{1,1} & u_{1,2} & \cdot & u_{1,n} \\ u_{2,1} & u_{2,2} & \cdot & u_{2,n} \\ \cdot & \cdot & \cdot & \cdot \\ \cdot & \cdot & \cdot & \cdot \\ u_{m,1} & u_{m,2} & \cdot & u_{m,n} \end{bmatrix} \begin{bmatrix} \sigma_1 & & \\ & \sigma_2 & \\ & & \cdot \\ & & & \sigma_r \end{bmatrix} \begin{bmatrix} v_{1,1} & v_{2,1} & \cdot & v_{n,1} \\ v_{1,2} & v_{2,2} & \cdot & v_{n,2} \\ \cdot & \cdot & \cdot & \cdot \\ v_{1,r} & v_{2,r} & \cdot & v_{n,r} \end{bmatrix}. \tag{20}$$

$$\sigma_1 > \sigma_2 > \ldots > \sigma_r \geq 0$$

Consider a real matrix Z to be of size m by n (denoted (m,n)) and rank r. Matrix Z can then be expressed as a product of the three unique matrices:

(1) Matrix U called the left-singular-vectors" (LSV) is an orthonormal matrix of size (m,r). The columns of this matrix are unity-norm vectors which are orthogonal to each other. This set of vectors serves as a basis for the column-space of matrix Z.

(2) Matrix Σ is a diagonal matrix (size (r,r)) that holds the singular values of Z as entries along its diagonal. The singular values are non-negative real numbers that can be arranged along the diagonal in a descending order.

(3) Matrix V called the right-singular-vectors (RSV) is an orthonormal matrix of size (n,r). The columns of this matrix (or the rows of V^T) are unity-norm vectors, which are orthogonal to each other. The set of these vectors serves as a basis for the row-space of matrix Z.

One should view this decomposition as a way of finding convenient orthogonal bases for both the column space and the row space of an arbitrary real matrix.

The SVD of a real matrix can alternatively be regarded as a spectral decomposition of any arbitrary real matrix Z. A generic real matrix Z of rank r can be expressed as a linear combination of r rank-one matrices as expressed in Equation (21).

$$
Z = \sigma_1 \begin{bmatrix} u_{1,1} \\ u_{2,1} \\ \cdot \\ \cdot \\ u_{m,1} \end{bmatrix} \begin{bmatrix} v_{1,1} \ v_{2,1} \ \cdot \ v_{n,1} \end{bmatrix} + \sigma_2 \begin{bmatrix} u_{1,2} \\ u_{2,2} \\ \cdot \\ \cdot \\ u_{m,2} \end{bmatrix} \begin{bmatrix} v_{1,2} \ v_{2,2} \ \cdot \ v_{n,2} \end{bmatrix} + \ldots + \sigma_r \begin{bmatrix} u_{1,n} \\ u_{2,n} \\ \cdot \\ \cdot \\ u_{m,n} \end{bmatrix} \begin{bmatrix} v_{1,r} \ v_{2,r} \ \cdot \ v_{n,r} \end{bmatrix}.
$$

(21)

$$\sigma_1 > \sigma_2 > \ldots > \sigma_r \geq 0$$

The practicality of this approach is that any real matrix Z can be approximated as a lower ranked matrix by using partial of its rows and columns basis. The proximity between the original matrix and the approximated one can be assessed by the evaluation of each of the matrix's norm. There is more than one way to measure the magnitude of a matrix (various norms). The preferable norm for the proposed CVSDR method is the *Frobenius* norm [23]. This norm is defined as the square root of the sum of all squares of the elements of the matrix. This norm can be expressed, with few algebraic passages, as the square root of the sum of all singular-values squares (Equation (22)).

$$\|Z\|_F \equiv \sum_{i=1}^{m} \sum_{j=1}^{n} \sqrt{(z_{i,j})^2} = \sqrt{\sigma_1^2 + \sigma_2^2 + \ldots + \sigma_r^2}.$$

(22)

The ability to approximate any arbitrary real matrix of rank r by an increasing sum of rank-one matrices is the essence of the dimensionality reduction concept. Reducing the long list of 36 corrected variables (Table 3) to a short and practical list of effective CVs for the level-flight performance is precisely based on this concept of dimensionality reduction.

SVD implementation for CV list refinement
The SVD theorem is used to identify which are the most effective CVs in representing the level-flight performance of a specific helicopter. One should regard this procedure in linear algebraic terms as finding an efficient orthogonal basis to represent the level-flight performance. A similar approach was presented by the authors for the problems of gas-turbine empirical models [13] and power required to hover [14]. This screening procedure is demonstrated using the MBB BO-105 helicopter flight-test data presented in Section 2. The procedure starts with filling matrix Z with numeral entries of all 36 CVs as measured for the level-flight sorties. For this demonstration 36 stabilised level-flight points measured in sorties 1, 2 and 3 are used. The columns of the matrix represent the various CVs (ψ_1^* to ψ_{36}^*) and the 36 rows represent the different test points measured. Next is to normalise all columns of Z to have a mean of zero and a variance of 1 as presented in Equation (23). Once matrix Z contains normalised columns it can be partitioned into the three unique matrices as per Equation (21).

$$\psi_i' = \frac{\psi_i^* - \overline{\psi_i^*}}{S_{\psi_i^*}}, i = 1, 2, \ldots, 35, 36.$$

(23)

The level-flight performance as appears in matrix Z is represented by all 36 CVs (ψ_1^* to ψ_{36}^*). However, not all CVs possess the same significance in representing the variance captured in the flight-test data. The singular values (σ_i) that appear along the main diagonal of matrix Σ in a descending order are key to understanding the level of importance each CV (i) holds. The conceptual interpretation of the SVD of Z for the specific problem of level-flight performance is illustrated in Fig. 9 and is further explained hereinafter.
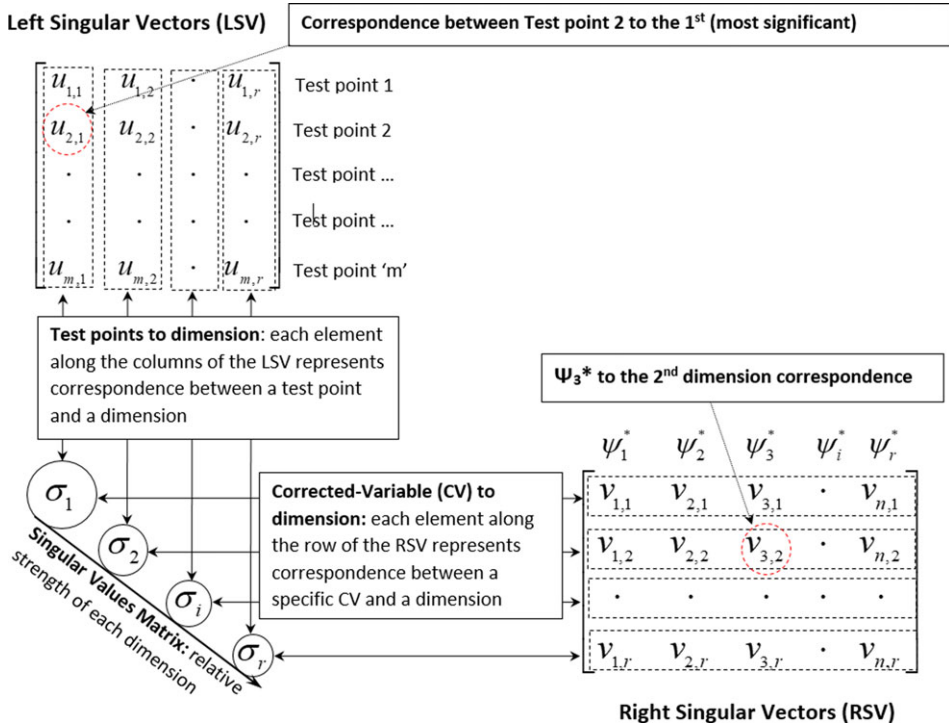
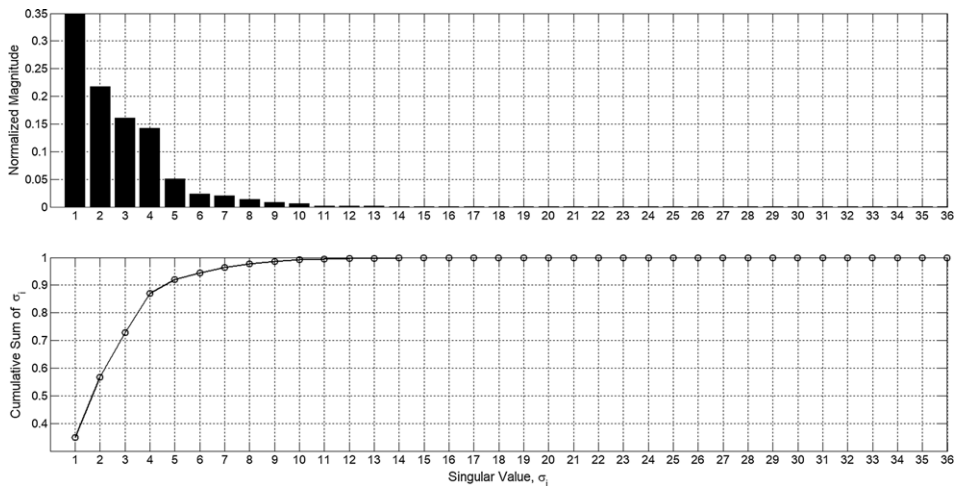**Figure 9.** *The conceptual interpretation of the SVD of matrix Z.*

Figure 10. *The singular-values of matrix Z (level-flight performance).*

The 36 singular values of matrix Σ are normalised as per Equation (24) and are presented in Fig. 10 alongside a cumulative-sum plot of all normalised singular values.

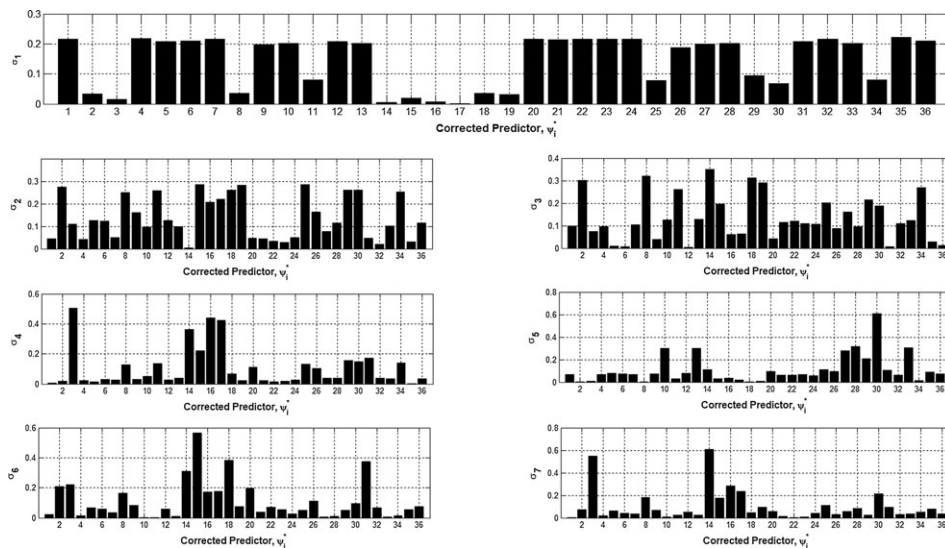$$\hat{\sigma}_i = \frac{\sigma_i}{\sum_{k=1}^{36} \sigma_k} i = 1, 2, \ldots, 35, 36. \tag{24}$$

Figure 11. *Correspondence between CVs and level-flight dimensions (rows of the RSV).*

One should deduce from Fig. 10 that the dimensionality of the level-flight problem can be significantly reduced from a 36-dimension problem to only a 7-dimension. In linear-algebraic terms it can be stated that the level-flight performance can be sufficiently described by a basis of only seven orthogonal CVs. The cumulative sum plot presented in Fig 10 indicates that 96.7% of the total variance in the flight-test data, as stored in matrix Z, can be presented by using the seven most significant CVs. Also indicated by Fig. 10, the most significant dimension of the level-flight performance problem holds 35% of the variance in the data. Comparing the *Frobenius* norm of matrix Z and its seventh order approximation (the combination of the first 7 rank-1 matrices) reveals a practically similar norm of the two; 34.986 for Z and 34.983 for the seventh order approximation.

The identity of the seven most important CVs is solely indicated by the RSV matrix. As illustrated in Fig. 9, each row of the RSV indicates the level of correspondence to a specific singular value or a dimension of the problem. For example, the first row of the RSV specifies the level of correspondence each one of the 36 CVs has to the first (and most significant) singular value. The second row of the RSV indicates the correspondence between all 36 CVs to the second most significant dimension of the problem, and so on. Since the dimensionality of the problem was reduced from 36 to 7, it is required to evaluate only the first seven rows of the RSV matrix. For this, the elements along the first seven rows of the RSV matrix are normalised as per Equation (25) and presented in Fig. 11. The significance of each CV towards the seven substantial dimensions of the level-flight performance is then concluded.

$$\hat{V}(i,j) = \frac{|V(i,j)|}{\sum_{j=1}^{36}|V(i,j)|} i = 1, 2, \ldots, 6, 7. \tag{25}$$

The LSV matrix has no significant role in the type of analysis addressed in this paper since it only indicates the level of correspondence between each one of the level-flight test points and the singular-values of Z. This type of correspondence between particular test points and the various dimensions of the level-flight performance was deemed irrelevant to the topic analysed.

The following conclusions can be drawn from Figs 10 and 11: (1) the first and most significant dimension of the level-flight performance holds for 35% of variance in the data and is best represented by $\psi_1{}^*$. This CV represents variance in power. (2) The second most significant dimension of the level-flight performance holds for 21.7% of variance in the data and is best represented by $\psi_2{}^*$. This CV represents the variance in gross weight of the helicopter. (3) The third dimension of the level-flight performance

holds for 16.1% of variance in the data and is best described by ψ_{14}^*. (4) The fourth dimension of the problem holds for 14.3% of variance in the data and is best represented by ψ_3^*. (5) The fifth dimension of the problem holds for 5.1% of variance in the data and is best represented by ψ_{30}^*. This ψ_{30}^* involves power and since the first dimension already yielded a power-based CV for the role of an independent CV for the physical problem in hand this CV was renounced. Next in line (non-power related) to best represent the fifth dimension were the two CVs ψ_{10}^* and ψ_{13}^* which could not be differentiated with respect to their representation of the fifth dimension. (6) The sixth dimension of the problem holds for 2.3% of variance in the data and is best represented by ψ_{15}^*. (7) the least significant dimension in the truncated list of seven dimensions holds for only 2% of variance in the data and is best represented by the same CV selected to represent the third dimension, which is ψ_{14}^*.

Finally, a ***conceptual*** empirical model to represent the level-flight performance of the MBB BO-105 helicopter, as resulted from the CVSDR method, can be stated as Equation (26). This relation involves six independent CVs and one power-based dependent CV.

$$\psi_1^* = f\left(\psi_2^*, \psi_{14}^*, \psi_3^*, \psi_{10}^*, \psi_{13}^*, \psi_{15}^*\right) \therefore \frac{P}{\delta\sqrt{\theta}} = f\left(\frac{W}{\delta}, \omega^2\sqrt{\theta}, \frac{\omega}{\sqrt{\theta}}, \frac{V_T}{\sqrt{\theta}}, \frac{V_T}{\omega}, \frac{X_{cg}}{R}\right). \tag{26}$$

3.3 Phase 3 – From a conceptual model into a practical empirical model

Once the most influential CVs of the level-flight performance problem are exposed, a practical empirical polynomial in the six independent CVs is pursued. The physical nature of the problem (Equation (1)) suggests a third order as the highest degree to represent the power in level flight. This puts a cap on the order of the empirical polynomials to be explored. As a guideline for simplicity the prospective polynomial needs to refrain from employing any cross-products of CVs as regressors. Numerous configurations involving the six independent CVs were evaluated for their power estimation accuracy using the 36 stabilised data points from the first three sorties specified in Table 1. The particular polynomial presented as Equations (27) and (28) was selected due to its best performance in representing the power measurements in the first three sorties, i.e. yielding the least values for the mean and the variance of the estimation errors. This empirical model is addressed hereinafter as Model 123 (M123) since it is based on flight-test data from sorties 1, 2 and 3.

$$\frac{P}{\delta\sqrt{\theta}} = \gamma_{1_{M123}}\left(\frac{W}{\delta}\right) + \gamma_{2_{M123}}\left(\frac{W}{\delta}\right)^2 + \gamma_{3_{M123}}\left(\omega^2\sqrt{\theta}\right) + \gamma_{4_{M123}}\left(\frac{\omega}{\sqrt{\theta}}\right) +$$
$$+ \gamma_{5_{M123}}\left(\frac{V_T}{\sqrt{\theta}}\right) + \gamma_{6_{M123}}\left(\frac{V_T}{\sqrt{\theta}}\right)^2 + \gamma_{7_{M123}}\left(\frac{V_T}{\sqrt{\theta}}\right)^3 + \gamma_{8_{M123}}\left(\frac{V_T}{\omega}\right) + \gamma_{9_{M123}}\left(\frac{V_T}{\omega}\right)^2$$
$$+ \gamma_{10_{M123}}\left(\frac{V_T}{\omega}\right)^3 + \gamma_{11_{M123}}\left(\frac{X_{cg}}{R}\right) + \gamma_{12_{M123}}, \tag{27}$$

$$\begin{Bmatrix} \gamma_{1_{M123}} \\ \gamma_{2_{M123}} \\ \gamma_{3_{M123}} \\ \gamma_{4_{M123}} \\ \gamma_{5_{M123}} \\ \gamma_{6_{M123}} \\ \gamma_{7_{M123}} \\ \gamma_{8_{M123}} \\ \gamma_{9_{M123}} \\ \gamma_{10_{M123}} \\ \gamma_{11_{M123}} \\ \gamma_{12_{M123}} \end{Bmatrix} = \begin{Bmatrix} -6.679 \\ 5.85 \times 10^{-4} \\ -19.475 \\ -1019.915 \\ 418.52 \\ -2.989 \\ 8.31 \times 10^{-3} \\ -19336.47 \\ 6189.634 \\ -742.462 \\ 116.372 \\ 102479 \end{Bmatrix} \therefore \textbf{M123}. \tag{28}$$
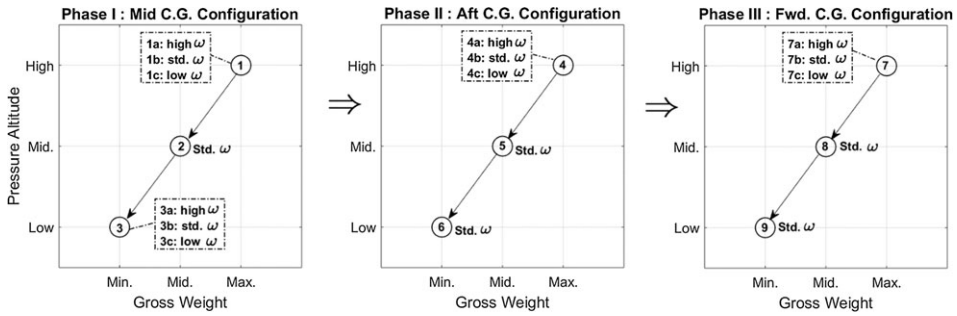
Figure 12. *CVSDR level flight performance sorties planning and execution sequence.*

3.4 The CVSDR method for level flight performance – Summary and practical guidance

A performance flight-testing campaign starts with a careful planning of the required sorties. The power required for level flight using CVSDR is no exception to this rule. The flight tester should plan for a set of level-flight speed runs to cover the applicable and required flight envelope. With the aim of establishing a sound data base to be analysed, the flight tester should gather level-flight performance that covers the entire range of airspeed (V_T), gross-weight (W), centre of gravity (Xcg), main-rotor angular speed (ω) and ambient air properties of pressure and temperature. Figure 12 provides a methodical approach for sorties planning and execution while using the CVSDR method. The flight-test campaign should be executed in three configuration-based phases. Each phase includes a set of various speed-runs (denoted as the numbers 1 to 9 in Fig. 12) conducted at various conditions of gross weight, altitude and main rotor angular speed. Every single speed-run should be conducted from the lowest practicable airspeed (hover if possible) to the highest attainable level flight airspeed, with about eight different intermediate airspeeds.

At each stabilised airspeed point, the flight-tester needs to gather all data needed to compute the corrected variables presented in Table 3. The flight-test campaign should start with a middle centre of gravity (cg) configuration (the left chart in Fig. 12), followed by an aft cg configuration (the middle chart in Fig. 12) and end with a forward cg configuration. The first sets of speed runs should be conducted at high altitude and high gross weight; this would extend the range of many weight-based corrected variables presented in Table 3. For helicopters that allow the crew to adjust the main rotor speed under standard procedures, few sets of speed runs shall be repeated three times for three distinct values of main rotor speed that span the governed range (see example denoted as 1a, 1b and 1c in Fig. 12). Note that by following the directions of Fig. 12 closely, the flight-test team are expected to acquire a database of 17 distinct speed runs, totaling about 136 stabilised level flight data points. This would constitute a sound database to be analysed. Succeeding the establishment of this database, the flight test data analysis should be conducted by following the sequential eight steps of Table 4. This table is intended to provide a practical, step-by-step guidance, to realise the three phases of the CVSDR method as discussed in Sections 3.1, 3.2 and 3.3 above.

4.0 Prediction accuracy achieved using the CVSDR method

The prediction accuracy achieved using the CVSDR method is evaluated hereinafter in a build-up manner. First, it is evaluated against the conventional flight-test method by using the flight test data from sorties 1 through 4, all conducted at the same targeted coefficient of weight. Next, the CVSDR method is challenged to predict level-flight performance of a new sortie (Sortie 5), which was conducted under arbitrary and varying (Cw). This evaluation is performed only for the purpose of challenging the CVSDR-based empirical model and to experiment up to what extent it can predict (extrapolate) the

Table 4. *The CVSDR data analysis for level flight performance – a step-by-step guidance*

Step	Task description & instruction
Phase 1 – Establish an applicable list of CVs to represent the level-flight performance (Para. 3.1)	
1	Compute all 36 CVs (Table 3) for each stabilised level-flight data point measured. There should be 136 stabilised data points, if all sorties of Fig. 12 were closely executed.
2	Arrange the computed CVs in a matrix form (this is matrix Z). The rows of Z should represent the different data points and columns of Z should represent the various CVs. If all sorties of Fig. 12 were closely executed, matrix Z should be of size 136×36.
Phase 2 – Screening for the most effective CVs using dimensionality reduction (Para. 3.2)	
3	Normalise all columns of matrix Z as per Equation (23) to have a zero mean and a variance equals one.
4	Decompose the ***normalised*** matrix Z into its three unique matrices (U, Σ and V) using a singular value decomposition (SVD) algorithm. Matrix U is also referred to as the left singular vectors (LSV), matrix Σ is called the singular values and matrix V is called the right singular vectors (RSV).
5	Normalise all singular values (entries along the main diagonal of matrix Σ) as per Equation (24). The normalised values represent the relative strength of the various dimensions exist in the data. Determine the number of ***significant*** dimensions involved in the specific level-flight performance data, based on the cumulative sum of the normalised singular values (as presented in Fig. 10).
6	Normalise the rows of matrix V^T (RSV) as per Equation (25). This normalisation calls for the absolute value of each element along the rows of RSV to be divided by the sum of all elements absolute values along the corresponding row of RSV.
7	Identify the most significant CVs of the specific level-flight performance analysed. The level of correspondence between each CV and an abstract dimension of the level-flight problem is illustrated in Fig. 9. Note that only the first significant rows of the normalised matrix V^T should be evaluated. The number of significant rows of V^T equals the number of significant dimensions retrieved in sequential Step 5 above. Example for this step is presented in Fig. 11.
Phase 3 – Forming a practical empirical model (Para. 3.3)	
8	Use the most significant CVs identified in sequential Step 7 to form a practical polynomial that uses the relevant CVs as regressors in this empirical model.

level-flight performance of the same helicopter but under arbitrary conditions. Note the empirical models retrieved using the conventional method in Section 2 (Equation (6)) are irrelevant for the prediction of Sortie 5. These empirical models represnt the level flight performance of the helicopter for a single and specific *Cw*, the one targeted in sorties 1 through 4. For Sortie 5, the comparison between the conventional and CVSDR methods is trivial since the conventional method immediately fails.

4.1 Prediction accuracy within the same coefficient of weight

The latter two phases of the CVSDR method, phases 2 and 3 as presented in Section 3, were repeated by utilising the three other combinations available from the flight-test data of sorties 1 through 4. An empirical model based on flight-test data from sorties 1, 3 and 4 (denoted M134) was used for the prediction of the power levels in Sortie 2. This empirical model, which employs nine distinct regressors and a constant, is presented in Equation (29) without the numeral coefficient. The same approach was
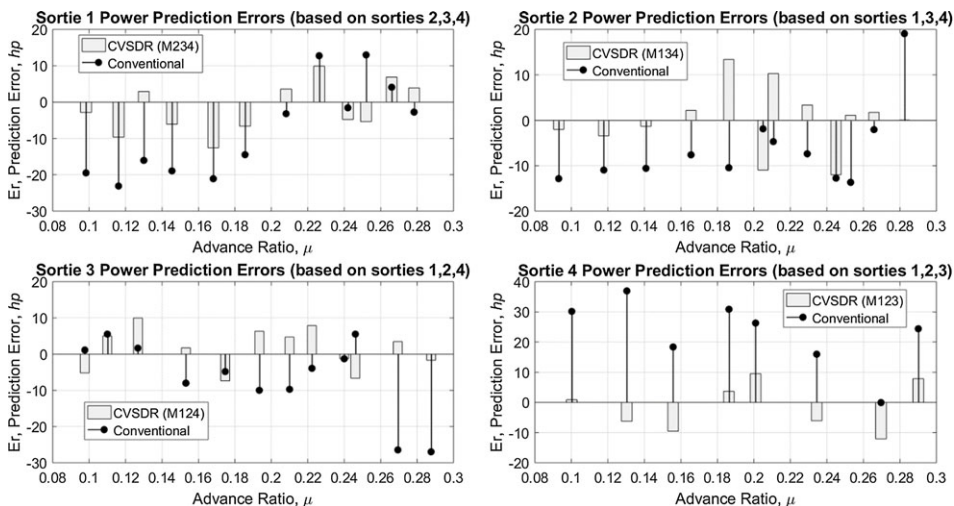
Figure 13. *Power prediction errors – conventional and CVSDR methods comparison.*

repeated for the derivation of M234 and M124 (empirical models based on sorties 2, 3, 4 and 1, 2, 4 accordingly) for power levels predictions of sorties 1 and 3, respectively. The two models, M234 and M124, employ (each) eight regressors and a constant and are presented in Equation (29). Mind that the four empirical models (M123, M134, M234 and M124) share many of the same regressors but are not exact. This is expected since they are based on slightly different flight test databases.

$$\frac{P}{\delta\sqrt{\theta}} = \gamma_1\left(\frac{W}{\delta}\right) + \gamma_2\left(\frac{W}{\delta}\right)^2 + \gamma_3\left(\omega^2\sqrt{\theta}\right) + \gamma_4\left(\frac{\omega}{\sqrt{\theta}}\right) +$$

$$+ \gamma_5\left(\frac{V_T}{\sqrt{\theta}}\right) + \gamma_6\left(\frac{V_T}{\sqrt{\theta}}\right)^2 + \gamma_7\left(\frac{V_T}{\sqrt{\theta}}\right)^3 + \gamma_8\left(\frac{V_T}{\omega X_{cg}}\right) + \gamma_9\left(\frac{X_{cg}}{R}\right) + \gamma_{10} \quad \textbf{M134}. \tag{29}$$

$$\{\textbf{M234}: \gamma_3 \equiv 0 \; \therefore \; \textbf{M124}: \gamma_4 \equiv 0\}$$

Power prediction errors were calculated for all four sorties in the same manner demonstrated by Equation (30), specifically for Sortie 4. Figure 13 presents these calculated prediction errors against their corresponding advance ratios. For comparison purposes, Fig. 13 includes the prediction errors obtained from the conventional flight-test method (cluster of sorties approach).

$$\bar{E}_r = P_i - \delta_i\sqrt{\theta_i}\left(\begin{array}{l}\gamma_{1_{M123}}\left(\frac{W}{\delta}\right)_i + \gamma_{2_{M123}}\left(\frac{W}{\delta}\right)_i^2 + \gamma_{3_{M123}}\left(\omega^2\sqrt{\theta}\right)_i + \gamma_{4_{M123}}\left(\frac{\omega}{\sqrt{\theta}}\right)_i + \gamma_{5_{M123}}\left(\frac{V_T}{\sqrt{\theta}}\right)_i + \gamma_{6_{M123}}\left(\frac{V_T}{\sqrt{\theta}}\right)_i^2 \\ + \gamma_{7_{M123}}\left(\frac{V_T}{\sqrt{\theta}}\right)_i^3 + \gamma_{8_{M123}}\left(\frac{V_T}{\omega}\right)_i + \gamma_{9_{M123}}\left(\frac{V_T}{\omega}\right)_i^2 + \gamma_{10_{M123}}\left(\frac{V_T}{\omega}\right)_i^3 + \gamma_{11_{M123}}\left(\frac{X_{cg}}{R}\right)_i + \gamma_{12_{M123}}\end{array}\right) \; \therefore \; i = 1, 2, \ldots, 8. \tag{30}$$

The superiority of the CVSDR over the conventional method is immediately evident from Fig. 13. Power prediction of Sortie 1 using M234 resulted in prediction errors that ranged from −12.6 hp (over-estimate) to 9.9 hp (underestimate). The prediction errors mean was −1.7 hp with a standard deviation of 7 hp. This compares to prediction errors ranging from −23.1 to 12.8 hp (averaged at −7.6 hp with a wide standard deviation of 13 hp) achieved by using the conventional method. Comparing the two methods for the other three sorties reinforces the prediction accuracy advantage of the CVSDR method: for Sortie 2, the CVSDR prediction errors averaged at 0.2 hp with a standard deviation of 7.3 hp as compared to a mean of −6.3 hp with a standard deviation of 9 hp, yielded by the conventional method. For Sortie 3, the respective comparisons were prediction error means of 1.4 and −6.4 hp in favour of the CVSDR and standard deviations of 5.8 and 10.8 hp in favour of the CVSDR. For Sortie 4, the CVSDR
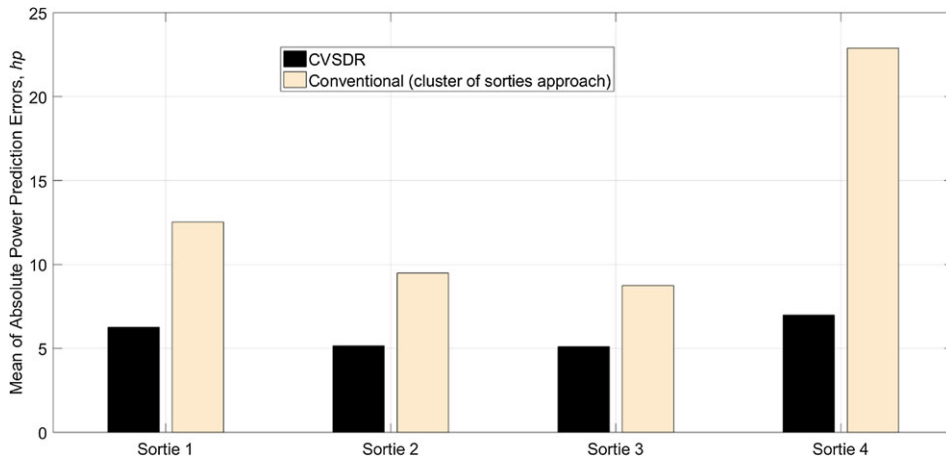
Figure 14. *Mean of power prediction errors – CVSDR and conventional methods comparison.*

method achieved a prediction error mean of only -1.5 hp, compared to an underestimation average of 22.9 hp. The CVSDR prediction errors for Sortie 4 were also less scattered as demonstrated by the two standard deviations (8.1 hp compared to 11.5 hp).

Figure 14 presents an alternative view of the data displayed in Fig. 13. The means of the ***absolute*** prediction errors for each sortie were calculated as per Equation (8) and are presented alongside the corresponding values retrieved from the conventional method (cluster of sorties approach). Once more, the CVSDR method performed better for this comparison. The means of absolute errors for sorties 1 through 4 were 6.3, 5.2, 5.1 and 7 hp accordingly. These means compare to 12.5, 9.5, 8.7 and 22.9 hp resulted from the conventional method.

Inferring from the particular case of the four sorties to the general case is realised by using the hypothesis testing, as demonstrated in Section 2 for the conventional method. The null hypothesis assigned is that ***on-average*** the power required for level flight as predicted by the CVSDR method does not differ from the true measured power by more than ± 4 hp (the least deviation noticeable to the BO-105 aircrew). This null hypothesis is tested against the alternative that ***on-average*** the CVSDR estimated power for level-flight differ by more than 4 hp (absolute value) from the actual power. The relevant test-statistic for this hypothesis testing is calculated per Equation (10). The symbol n represents the number of sorties and S stands for the standard deviation of the averaged power prediction errors, calculated per Equation (8) and presented in Fig. 14. The test statistic was fairly large (4.11), mainly due to the relative low standard deviation. Inferential statistical analysis shows the probability of making a Type-I error by rejecting the null hypothesis is very small (1.3%), hence does not support the null hypothesis. On average and at the accustomed 95% confidence level, the CVSDR power predictions deviate from the actual measured power by ± 4.8 hp. Although above the 4 hp threshold noticeable to the BO-105 crew, this average prediction error is about 17% lower than the ± 5.8 hp achieved using the conventional method.

The correlation coefficient between the prediction errors and the advance ratio was calculated for all four sorties per Equation (9). Figure 15 presents these coefficients accompanied with those obtained from the conventional method, *cluster of sorties approach*. It is evident the CVSDR prediction errors do not significantly correlate to the advance ratio. As explained in Section 2, any correlation coefficient above 0.58 (absolute value) for sorties 1 through 3, and above 0.71 for Sortie 4 indicates a statistically significant correlation. It can be concluded that based on flight-test data from all four sorties, **the power prediction accuracy obtained from the CVSDR method is not related to the advance ratio. Similar accuracy level is expected from the CVSDR method regardless of the corresponding advance-ratio.**

Table 5. *Summary of flight-test conditions for Sortie 5*

Gross weight* [Lbs.]	Long. C.G.* [In.]	Pressure altitude* [ft.]	Ambient temp. [°C]	Cw range* [x10⁻³]	Main rotor speed*[RPM]
3,920–4,080	125.6–125.8	5,980–6,050	8	4.81–4.95	421–425

* values represent the range of change during the sortie.
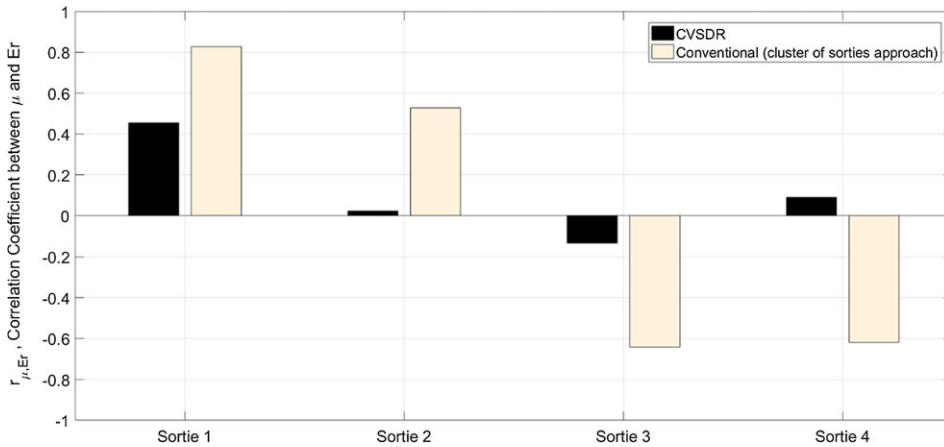
Figure 15. *Prediction errors to advance-ratio correlation (CVSDR and conventional methods).*

4.2 Prediction accuracy for a different coefficient of weight

One might wonder whether the adequate performance of the CVSDR method was made possible due to the fact the power estimations were made for the same coefficient of weight. For this, another sortie (number 5) was conducted under different values of coefficient of weight as specified in Table 5. Sortie 5 was executed ***without*** the cumbersome restriction imposed by the conventional method for maintaining a constant coefficient of weight and a constant main rotor speed while gathering the power required to sustain level flight at various airspeeds. The coefficient of weight varied between 4.8×10^{-3} to 4.95×10^{-3} and was significantly different from the value maintained constant during the first four sorties (5.79×10^{-3}).

The four empirical models originated from the CVSDR method were used to predict the power levels of ten stabilised data points of Sortie 5. These empirical models are M123 defined in Equations (27) and (28), M234, M134 and M124 specified in Equation (29). Prediction errors were calculated by subtracting the predicted power from the measured value; this way, a positive error represents an underestimation of the actual measured power. All power estimation errors for Sortie 5 are presented in Fig. 16 against the appropriate advance ratio. This figure also includes a presentation of the average estimation error of the four models for each data point.

As expected, all four empirical models provided adequate prediction levels, even for different and varying values of coefficient of weight. Prediction errors ranged from −11.1 to 10.1 hp for M134, −12.4 to 9.1 hp for M234, −9 to 12 hp for M124 and from −10.6 to 8.7 hp for M123. The prediction-error means were all close to zero (−0.9, −1.3, −0.7 and −0.4 hp for M134, M234, M124 and M123 accordingly) with relatively narrow standard deviations of 7.3, 8.6, 6.8 and 9.8 hp, respectively. Hypothesis testing at the 95% confidence level shows no statistically significant difference between the prediction performances of all four empirical models. Moreover, no statistical significance was found between the performance of each empirical model when acted on sorties 1 to 4 (constant Cw) or when acted on Sortie 5. That means one can expect adequate prediction performance when using the CVSDR method for extrapolating to a different coefficient of weight.
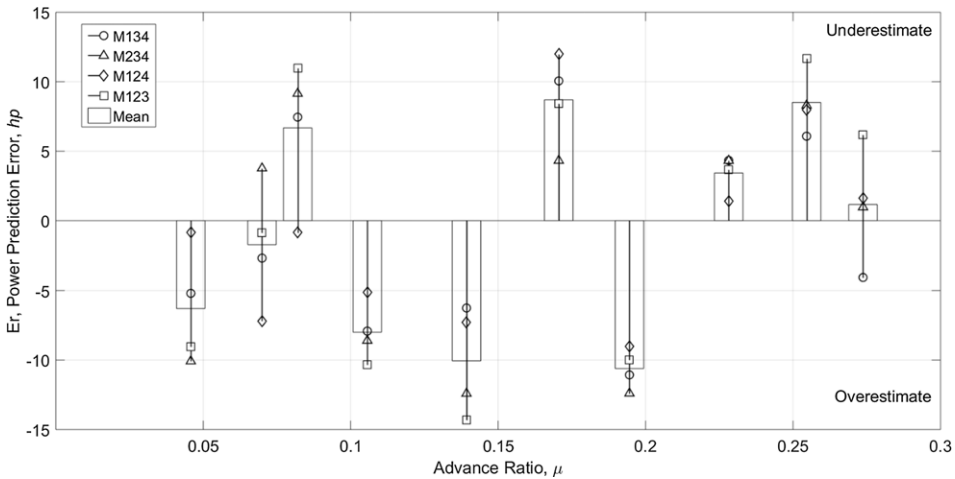
Figure 16. *Power prediction errors for Sortie 5 using the CVSDR method.*

The correlation coefficients (r) between the power-prediction errors of each empirical model and the advance-ratio were calculated per Equation (9). The values were significantly low; 0.17 for M134, 0.25 for M234, 0.42 for M124 and 0.41 for M123. For the specific number of data points in Sortie 5 (10) and the accustomed 95% confidence level, only a value of 0.632 and above indicates a significant correlation between the two variables. It can be concluded that based on flight-test data of Sortie 5 no significant correlation was found between the power prediction errors using all four empirical models (M134, M234, M124 and M123) and the advance ratio.

5.0 A comparison between the conventional and the CVSDR methods

The conventional flight-testing method for level-flight performance is based on a simplification of the physical problem and comprises several drawbacks that affect the accuracy and efficiency of the method. This section draws a comparison between the conventional and the proposed CVSDR methods by dwelling on each one of the conventional method's drawbacks specified in the introduction.

First and foremost, the prediction accuracy expected from each method is different. Figure 13 shows a comprehensive comparison between the prediction errors attained from each method for all four sorties, totaling 44 flight-test data points. Figure 14 compares the two methods by presenting the mean of the absolute prediction errors for each sortie. The superiority of the CVSDR method over the conventional method is clear. The conventional method was able to generate average absolute prediction errors of 12.5, 9.5, 8.7 and 22.9 hp compared to 6.3, 5.2, 5.1 and 7 hp (respectively) yielded by the CVSDR method. Statistical analysis shows that *on-average* (at the 95% confidence level) the CVSDR power predictions deviate by up to 4.8 hp (absolute value) from the actual measured power. The corresponding deviation obtained from the conventional method is 5.8 hp, an increase of nearly 21%.

The prediction errors generated from the conventional method were significantly correlated with the advance-ratio whereas the CVSDR method demonstrated prediction accuracy with no correlation to the advance ratio. This correlation between the prediction error and the advance ratio might suggests there is a latent phenomenon related to the advance ratio, which is missed by the conventional method and the empirical model it yields.

The conventional method is aimed at constant coefficient of weight data. As such, the empirical models retrieved from the first four sorties were useless for the predictions of Sortie 5. The proposed CVSDR method is more versatile in this manner and was successfully used for the predictions of Sortie 5. Besides

the versatility aspect, the constant coefficient of weight restriction makes the execution of the conventional flight-test method cumbersome and more time consuming compared to the CVSDR method. As described in Section 2.1, the conventional method requires the flight-test crew to continuously calculate and adjust the cruise altitude to maintain a constant coefficient of weight. For a small-sized and light helicopter, this inflates the flight time required for each data point from about 2min to about 5min. For large and heavy helicopters this inflation rate is even expected to increase more. On a flight-test campaign that requires five different coefficients of weight, each including eight different airspeeds, the CVSDR method is expected to save about 2h of flight time. This is about 60% reduction in the flight-test duration required by the conventional method. Moreover, losing the requirement for a continuous adjustment of the cruise altitude based on the helicopter weight can free up valuable crew resources and promote flight safety.

There are two approaches of maintaining a constant (Cw during speed runs. The first is to keep a constant ratio of weight over relative density (W/σ) and a constant main-rotor angular speed. This approach is discussed Section 2.1 and thoroughly demonstrated in Section 2.2. The second approach for maintaining a constant coefficient of weight was not demonstrated in the paper but is discussed in Section 2.1. This second approach requires the flight tester to maintain a constant ratio of static ambient temperature (T_a) over the main-rotor angular speed squared (Ω^2) during the speed-runs. These requirements dictate a continuous involvement of the flight-test crew with the main rotor speed. For the first approach of constant main rotor speed the crew need to continuously apply fine-tuning, either to compensate for a non-perfect control system (M/R speed governor) functioning, or even to override an inherent scheduling profile dictated by the govern control laws. When executing the second approach the flight tester involvement with main rotor speed adjustments is even more challenging since they need to maintain a constant value of Ta/Ω^2. Besides the fact this main rotor speed continuous manipulation during the test imposes inconvenience on the crew, there are types of helicopters (the MD-902 Explorer as an example) that do not allow the crew to adjust the main rotor speed under standard procedures. For these types of helicopters, a *precise* execution of the conventional level-flight performance testing method is questionable, and undesirable scatter in the data is almost inevitable. The CVSDR method does not force the test crew to follow any kind of main rotor speed profile, or to keep it fixed. Any variation in the main rotor speed regardless of its initiation source (automatically by the control system or manually by the flight-test crew) can be used as a valid flight-test data point. That said, the flight tester should be reminded that flight-test data should be collected throughout the flight envelope of the aircraft. For this reason, performance data should be collected for the entire range of main rotor angular speed under normal operations (as presented in Fig. 12).

Another drawback inherent to the conventional method and efficiently addressed by the proposed CVSDR method is the influence of the centre -of gravity on the power required for level flight. As mentioned in the introduction, migration of the centre of gravity can affect the helicopter attitude, hence alter the drag frontal area of the helicopter. Through this mechanism the power required to sustain level flight is affected as well. Unlike the conventional method that neglects this influence, the CVSDR method identified a corrected variable (ψ_{15}^*) that conveys the effect of centre of gravity migration into the empirical power model. For the specific type of helicopter tested and the limited scope of tests, this centre of gravity was identified as the sixth concept in the data (σ_6), responsible for 2.3% of variance in the data (as presented in Fig. 11). Note that the specific data analysed covers a limited centre of gravity travel range (between longitudinal stations 123.5 and 124.4 inch as per Table 1), which represents only 6.4% of the allowed longitudinal centre of gravity of the BO105 helicopter. Expanding the flight-test database to include level flight performance data measured under a larger centre of gravity travel range might have resulted in a larger significance of the relevant corrected variable (ψ_{15}^*).

The conventional method is bounded by the high-speed approximation, meaning it is relevant only for airspeeds in which the induced velocity through the main-rotor disk is negligible as compared to the airspeed the helicopter flies at. This makes the conventional method irrelevant for modeling and estimating power required in the low-airspeed regime. The CVSDR method is by no means bound by this high-speed approximation and is indeed relevant for the low-airspeed regime. As seen in Fig. 16,

the CVSDR method was also applied to the low-airspeed regime and provided adequate power estimations in this regime. Three power estimations were made for the advance ratios of 0.05, 0.07 and 0.08 representing true-airspeeds of 19, 30 and 35Kn, respectively. Those estimations were at a similar accuracy level as achieved for the high-speed regime. Nevertheless, statistical analysis for Sortie 5 and the CVSDR method showed no significant correlation between the power prediction errors and the advance ratio.

6.0 Conclusions

The conventional flight-test method to evaluate helicopter performance in level flight includes many drawbacks that seriously compromise its accuracy and its execution efficiency. The proposed CVSDR method aims at addressing those downsides of the conventional flight-test method. The CVSDR method showed great potential as it was used successfully with level-flight test data obtained from a MBB BO-105 helicopter. The power prediction accuracy achieved using the CVSDR method was nearly 21% better than the level of accuracy yielded from the conventional flight-test method. Moreover, the CVSDR method does not require the test crew to follow a strict and binding flight scheduling, as mandated by the conventional method. This potentially makes the CVSDR more efficient and time conserving. The CVSDR is estimated to reduce flight-time for data points gathering by at least 60%. The CVSDR method is not restricted by the high-speed approximation and is therefore relevant to the low-airspeed regime, as opposed to the conventional flight-test method. This low-airspeed regime relevancy can potentially bridge the empirical-modelling gap between the two most important flight regimes of the helicopter – the hover, and the level flight. Although demonstrated using flight-test data from a BO-105 helicopter, the CVSDR method is applicable for any other type of conventional helicopter in level flight.

References

[1] 1. Porterfield, J.D., and Alexander, W.T. Measurements and evaluation of helicopter flight loads spectra data, *J. Amer. Helicop. Soc.*, July 1970, **15**, (3), pp 22–34(13).

[2] U.S. Department of Transportation, Federal Aviation Administration, Certification of Normal Category Rotorcraft, AC 27-1B, Change 3, Subpart C, Strength Requirements, AC 27.571, September 2008.

[3] Leishman, J.G. *Principles of Helicopter Aerodynamics*, 2nd ed., Cambridge University Press, 2006, Chap. 5.

[4] Prouty R.W. Helicopter Performance Stability and Control, Krieger Publishing Company Malabar Florida, 1989, Chap. 4.

[5] U.S. Naval Test Pilot School, Flight Test Manual, USNTPS-FTM-No. **106**, Rotary Wing Performance, Naval Air Warfare Center, Patuxent River, Maryland, 31 December 1996, Chapter 7.

[6] Cooke, A.K. and Fitzpatrick, E.W.H. *Helicopter Test and Evaluation*, 1st ed., AIAA Education Series, 2002, Chap. 3.

[7] Stepniewski, W.Z. and Keys, C.N. Rotary Wing Aerodynamics, Two Volumes Bounded as One, Dover Publication, Inc., New York, 1984, Chap. 3.

[8] Nagata, J.I., Piotrowski, J.L., Young, C.J., et al. Baseline Performance Verification of the 12th Year Production UH-60A Black Hawk Helicopter. *Final Report, US Army Aviation Engineering Flight Activity*, Edwards AFB, California, USA, January 1989.

[9] Buckanin, R.M., Kelly, W.A., Webre, J.L., et al. Level Flight Performance Evaluation of the UH-60A Helicopter with the Production External Stores Support System and Ferry Tanks Installed. Final Report, US Army Aviation Engineering Flight Activity, Edwards AFB, California, USA, September 1986.

[10] Belte, D. and Stratton, M.V. Fuel conservation evaluation of U.S. Army helicopters, Part 4, OH-58C flight testing, Final Report, US Army Aviation Engineering Flight Activity, Edwards AFB, California, USA, August 1982.

[11] Boirun, B.H. Generalizing Helicopter Flight Test Performance Data (GENFLT), *The 34th Annual National Forum of the American Helicopter Society*, May 1978.

[12] Arush, I. and Pavel, M.D. Helicopter gas turbine engine performance analysis: A multivariable approach, *Proc. Inst. Mech. Eng. G: J. Aerosp. Eng.*, 2017; **223**, pp 837–850. https://doi.org/10.1177/0954410017741329

[13] Arush, I., Pavel, M.D. and Mulder, M. A singular values approach in helicopter gas turbine engine flight testing analysis, *Proc. Inst. Mech. Eng. G: J. Aerosp. Eng.*, April 2020. https://doi.org/10.1177/0954410020920060

[14] Arush, I., Pavel, M.D. and Mulder, M. A dimensionality reduction approach in helicopter hover performance flight testing, *J. Amer. Helicop. Soc.*, 2022, **67**, (032010). https://doi.org/10.4050/JAHS.67.032010

[15] Leishman, J.G. *Principles of Helicopter Aerodynamics*, 2nd ed., Cambridge University Press, 2006, Chap. 6.

[16] Prouty, R.W. Helicopter Performance Stability and Control, Krieger Publishing Company Malabar Florida, 1989, Chap. 3.

[17] Noonan, K.W. and Bingman, G.J. Two-Dimensional Aerodynamic Characteristics of Several Rotorcraft Airfoils at Mach Numbers from 0.35 to 0.9, NASA TM X-73990, Langley Research Center, Virginia, January 1977.

[18] Guttman, I., Wilks, S., and Hunter, J. *Introductory Engineering Statistics*, 2nd ed., John Wiley & Sons, Inc., New York, 1971, Chap. 10.

[19] Kreyszig, E. *Advanced Engineering Mathematics*, 3rd ed., John Wiley & Sons, Inc., New York, 1972, Chap. 19.

[20] Buckingham, E. On physically similar systems; illustrations of the use of dimensional equations, *Phys. Rev.*, 1914, **IV**, (4), pp 345–376, https://doi.org/10.1103/PhysRev.4.345

[21] Knowles, P. *The Application of Non-dimensional Methods to the Planning of Helicopter Performance Flight Trials and Analysis Results*, Aeronautical Research Council ARC CP 927, 1967.

[22] Strang, G. *Introduction to Linear Algebra*, 4th ed., Thomson Brooks/Cole, Belmont, CA, 2006, Chap. 6

[23] Horn, R.A. and Johnson, C.R. *Matrix Analysis*, 2nd ed., Cambridge University Press, New York, NY, 2012, Chap. 5